Effects of partial coherence on the scattering of x rays by matter

S. K. Sinha
Advanced Photon Source, Argonne National Laboratory, 9700 South Cass Avenue, Argonne, Illinois 60439

M. Tolan
Institut für Experimentalphysik der Universität Kiel, Leibnizstraße 19, D-24098 Kiel, Germany

A. Gibaud
Faculté des Sciences, Université du Maine, 72017 Le Mans Cedex, France
(Received 10 April 1997)

We discuss the scattering of x rays by matter using the Huygens-Fresnel method, i.e., in the kinematic regime. We derive expressions for how the mutual coherence function (MCF) of the scattered radiation defined across an exit aperture, arises from the MCF of the incident radiation across the entrance aperture and the electron density distribution of the scatterer, and in particular calculate the intensity measured in a detector placed behind the exit aperture as a function of the nominal wave vector transfer **q**. We discuss the exact relationship between this intensity function and the usual density-density correlation function of the scatterer, and discuss the relationship between coherence and instrumental resolution effects in various regimes. The Fraunhofer and Fresnel regimes are distinguished and the incoherent and coherent limits are discussed. We illustrate the results with explicit calculations for (a) Bragg reflections from crystals and (b) scattering from surfaces. [S0163-1829(98)06606-5]

I. INTRODUCTION

With the advent of high-brilliance synchrotron x-ray sources, it is now possible to obtain intense x-ray beams possessing a high degree of coherence. Several experiments have been recently carried out demonstrating the coherence properties of such beams, such as Fraunhofer diffraction patterns[1–3] and the observation of speckle patterns,[4,5] and their fluctuations in time, or intensity fluctuation spectroscopy (IFS).[6] However, most experiments are in practice carried out with radiation that is only partially coherent, and a quantitative understanding of the observed diffraction or speckle patterns depends on a proper theory for incorporating the effects of partial coherence on the scattering.

There have been several discussions of the diffraction of partially coherent radiation by *two-dimensional* apertures in the optical literature,[7] and the resulting formulation has been used to determine the mutual coherence function (MCF) of a soft x-ray laser source.[8] There have also been several measurements, using interferometry, of the coherence functions of partially coherent *neutron* beams.[9] Pusey[10] has discussed, in connection with IFS for visible light, the statistical properties of the light scattered by a fluctuating three-dimensional system, in terms of the correlation function of the incident light at the sample position, and in the far-field limit (i.e., neglecting detector resolution function effects), and assuming that the coherence length of the incident light inside the sample is much larger than correlation lengths within the sample.

Most treatments of the effects of finite beam divergence, energy spread, etc., use the resolution function folding procedure, i.e., the observed intensities are calculated in terms of a convolution of the actual scattering function $S(\mathbf{q})$ with an instrumental resolution function $\tilde{R}(\mathbf{q})$.[11–14] The real space representation of $\tilde{R}(\mathbf{q})$, i.e., its Fourier transform, is related to the coherence volume so that coherence lengths and resolution widths are regarded as conjugate quantities. This treatment is valid only in the limit when (a) the sample sees a completely *incoherent* source (note that even radiation from such a source may develop a finite degree of coherence at the sample position, if the latter is sufficiently far away from the source) and (b) we are in the far-field (Fraunhofer) diffraction regime. We note that the conditions for Fraunhofer diffraction are much more stringent for x-rays than for light, so that unless the aperture distances from the sample are very large, we must use Fresnel rather than Fraunhofer diffraction theory.[15]

In practice, beams of radiation falling on samples have encountered several optical elements on their way from the source, e.g., monochromators, mirrors, slits, etc., and thus it is often more useful to work in terms of the statistical properties, i.e., the mutual coherence function of the radiation, across the last aperture before the sample and calculate how the MCF is propagated via the scattering across an outgoing beam aperture and also the intensity in a detector behind this last aperture (see Fig. 1). The only restriction we make is that the distances L_1, L_2 from the sample to the incoming and outgoing apertures are sufficiently large compared to the sample and aperture dimensions that only terms up to *second* order need to be considered in the ratios of the latter to the former. Calculations for the scattering including second order terms have been carried out by Durbin[16] in connection with diffraction of a curved wave front by a crystal. Our calculations are valid in both the Fraunhofer and Fresnel regimes for diffraction, the conditions for which will be discussed explicitly. We find that the result for the observed intensity is in general more complicated than that given by the simple resolution-function folding procedure, except in

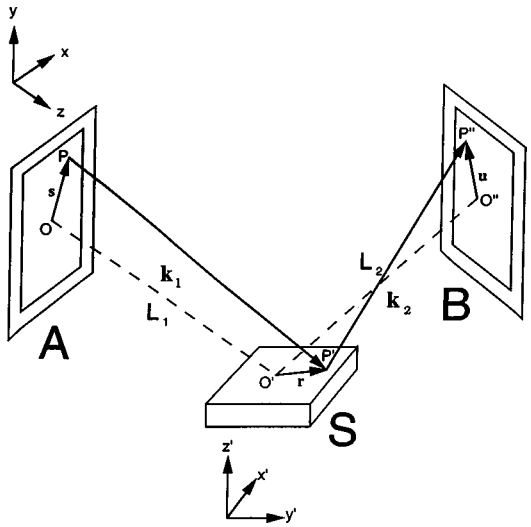

FIG. 1. Schematic view of the scattering geometry. L_1 is the distance between aperture A and the sample S, and L_2 the distance between the sample and the outgoing aperture B. The laboratory fixed coordinate system is given by (x,y,z), where (x,y) are along the dimensions of aperture A and z is along the mean direction $\hat{\mathbf{k}}_1$ of the incident radiation. The mean outgoing beam direction is $\hat{\mathbf{k}}_2$. The coordinates (x',y',z') with x' along x (out-of-plane direction), z' the direction perpendicular to the sample surface, and y' the surface in-plane direction define the more convenient surface-fixed system.

the limits referred to above, and we shall discuss these limits and also what happens in the opposite limit of complete coherence. We shall also discuss the application to the particular cases of Bragg reflection from a crystal, and scattering from a surface.

At this stage, it is worth recapitulating some well-known results of x-ray scattering theory in the kinematic (i.e., Born approximation). Consider a system described in terms of an electron density function $\varrho(\mathbf{r})$ placed in a perfectly monochromatic and collimated x-ray beam (single incident wave vector $\mathbf{k}_1$). The differential cross section for scattering is given by

$$\frac{d\sigma}{d\Omega}=P_1\left(\frac{e^2}{mc^2}\right)^2 S_0(\mathbf{q}), \tag{1}$$

where (e^2/mc^2) is the Thompson scattering length of the electron and P_1 is the Lorentz factor:

$$\mathbf{q}=\mathbf{k}_2-\mathbf{k}_1, \tag{2}$$

where $\mathbf{k}_2$ is the outgoing wave vector, and

$$S_0(\mathbf{q})=\int\int d\mathbf{r}\, d\mathbf{r}'\langle\varrho(\mathbf{r})\varrho(\mathbf{r}')\rangle_T \exp\{i\mathbf{q}\cdot(\mathbf{r}'-\mathbf{r})\}, \tag{3}$$

where we have assumed that the measurement is done over a long enough period of time T that we can make a *time average* of the correlation function inside the integral. We may also write

$$S_0(\mathbf{q})=\langle\tilde{\varrho}(\mathbf{q})\tilde{\varrho}^*(\mathbf{q})\rangle_T, \tag{4}$$

where

$$\tilde{\varrho}(\mathbf{q})=\int d\mathbf{r}\ \varrho(\mathbf{r})\exp(-i\mathbf{q}\cdot\mathbf{r}). \tag{5}$$

The tilde is henceforth used to denote the Fourier transform of the corresponding function without the tilde. Note that we have *not* taken any statistical ensemble averages in the above equations, as is normally done, since we are considering a *particular* realization of a sample in a *perfectly* coherent beam. If the sample is nonergodic, i.e., has builtin static randomness or disorder, $\langle|\tilde{\varrho}(\mathbf{q})|^2\rangle_T$ will possess sharp and random fluctuations about some particular average function, giving rise to the phenomenon of ''speckle.'' The width in q space of such speckles will typically be of the order π/D, where D is a typical sample dimension. They may be either distributed randomly (as in a sample with no spatial order at all) or clustered in regions of reciprocal space of width π/l, where l is a typical size of an ordered region. If on the other hand, the system is *ergodic*, with fluctuation time scales very short compared to the total integrated counting time T (e.g., a normal liquid), the *time average* is equivalent to an *ensemble average* and we may replace $\langle|\tilde{\varrho}(\mathbf{q})|^2\rangle_T$ by the usual ensemble average symbol $\langle|\tilde{\varrho}(\mathbf{q})|^2\rangle$. In this case, even for completely coherent radiation, there is no speckle. Instead, what is observed is a smooth function $S(\mathbf{q})$ calculated in the usual way by statistical mechanical methods.

For conventional scattering experiments, the diffuse scattering from disordered solids, rough surfaces, etc., does not usually exhibit speckle but also gives a smooth $S(\mathbf{q})$, which is in accordance with an ensemble average, notwithstanding the fact that the disorder in such systems is nonergodic. There are two ways to understand this. The first is a ''resolution function'' smearing of the speckle pattern in reciprocal space. In this picture, Eq. (1) is *folded* with an instrumental resolution function as if a whole series of beams (with a distribution of energies and incident and scattered directions) *independently* (i.e., incoherently) scatter from the sample, thus giving for the observed intensity at nominal wave vector transfer $\mathbf{q}$ (assuming unpolarized radiation)

$$I(\mathbf{q})=P_1\left(\frac{e^2}{mc^2}\right)^2\int \mathbf{K}S_0(\mathbf{K})\tilde{R}(\mathbf{q}-\mathbf{K}), \tag{6}$$

where $\tilde{R}(\mathbf{K})$ is the instrumental resolution or acceptance. This smearing out of the speckles is equivalent to an *average* over many *regions* of the sample, since by the convolution theorem and Eq. (3) (dropping the average over T, i.e., we assume for the moment systems which are static)

$$I(\mathbf{q})=P_1\left(\frac{e^2}{mc^2}\right)^2(2\pi)^3\int\int d\mathbf{r}\, d\mathbf{r}'\varrho(\mathbf{r})\varrho(\mathbf{r}')R(\mathbf{r}'-\mathbf{r}) \times\exp\{i\mathbf{q}\cdot(\mathbf{r}'-\mathbf{r})\}, \tag{7}$$

where $R(\mathbf{r})$ is the Fourier transform of $\tilde{R}(\mathbf{K})$, which acts as a cutoff function in real space, and we may consider it as defining a ''coherence volume.'' If this real-space cutoff is much smaller than the total sample volume, Eq. (7) is equivalent to the Fourier transform of a correlation function of $\varrho(\mathbf{r})\varrho(\mathbf{r}')$ averaged (on length scales equal to this cutoff) over the entire sample.

The second way to understand the smoothing is in terms of finite *coherence volumes* for the radiation in the sample. Let us assume that these are centered at positions $\mathbf{R}_l$ throughout the volume of the sample and are defined in terms of some (three-dimensional) real-space cutoff function $P(\mathbf{r})$. The *intensity* I_l of the scattering from the volume centered at $\mathbf{R}_l$ is given by

$$I_l(\mathbf{q}) = P_1\left(\frac{e^2}{mc^2}\right)^2 \left| \int d\mathbf{r}\ \varrho(\mathbf{r}) P(\mathbf{r}-\mathbf{R}_l) \exp(-i\mathbf{q}\cdot\mathbf{r}) \right|^2, \tag{8}$$

and we must sum these *intensities* over all such volumes, since they scatter incoherently from each other. Thus we obtain

$$I(\mathbf{q}) = P_1\left(\frac{e^2}{mc^2}\right)^2 \sum_l \left| \int d\mathbf{r}\ \varrho(\mathbf{r}) P(\mathbf{r}-\mathbf{R}_l) \exp(-i\mathbf{q}\cdot\mathbf{r}) \right|^2. \tag{9}$$

Writing $\varrho(\mathbf{r})$ and $P(\mathbf{r})$ in terms of their Fourier transforms, Eq. (9) is equivalent to

$$I(\mathbf{q}) = P_1\left(\frac{e^2}{mc^2}\right)^2 \int\int d\mathbf{K}\, d\mathbf{K}' \widetilde{\varrho}(\mathbf{K}) \widetilde{\varrho}^*(\mathbf{K}') \widetilde{P}(\mathbf{q}-\mathbf{K}) \times \widetilde{P}^*(\mathbf{q}-\mathbf{K}') \sum_l \exp\{i(\mathbf{K}-\mathbf{K}')\cdot\mathbf{R}_l\}. \tag{10}$$

For a large enough set of $\mathbf{R}_l$, the sum over l yields the condition $\mathbf{K}=\mathbf{K}'$ and in this limit,

$$I(\mathbf{q}) = P_1\left(\frac{e^2}{mc^2}\right)^2 \int d\mathbf{K}\ \widetilde{\varrho}(\mathbf{K}) \widetilde{\varrho}^*(\mathbf{K}) \widetilde{P}(\mathbf{q}-\mathbf{K}) \widetilde{P}^*(\mathbf{q}-\mathbf{K}), \tag{11}$$

which is identical to the form of Eq. (6) if $|\widetilde{P}(\mathbf{K})|^2$ is identified with the ''resolution function'' $\widetilde{R}(\mathbf{K})$. Thus in this *incoherent* limit (the coherence volume is much smaller than the sample volume) the conventional method of simply folding the true $S_0(\mathbf{q})$ with a resolution function in reciprocal space becomes correct, and the resultant scattering provides a reasonable approximation to an ensemble average, even though the experiment has involved a single realization of the sample. (For this to be true, the range of density correlations within the sample must also be much smaller than the sample size.)

Equation (6) has been traditionally used by researchers in x-ray scattering to obtain statistically averaged $S(\mathbf{q})$ functions for the system studied by ''unfolding'' the resolution function or by fitting. However, most x-ray radiation (whether emitted from an incoherent source or not) possesses a finite degree of coherence by the time it is incident on the sample and it is worth reanalyzing the expression for the observed intensity along the lines that researchers in optics have followed. As we shall see, when this is done, Eq. (7) must be replaced by

$$I(\mathbf{q}) = P_1\left(\frac{e^2}{mc^2}\right)^2 \int\int d\mathbf{r}\, d\mathbf{r}' \varrho_F(\mathbf{r}) \varrho_F^*(\mathbf{r}') R(\mathbf{r}',\mathbf{r}) \times \exp\{i\mathbf{q}\cdot(\mathbf{r}'-\mathbf{r})\}, \tag{12}$$

where $\varrho_F(\mathbf{r})$ is *not* the physical electron density but what we term the Fresnel electron density which is $\varrho(\mathbf{r})$ multiplied by a (complex) phase factor that depends on the directions of the incident and scattered beams, and the function $R(\mathbf{r}',\mathbf{r})$ does *not* depend only on the separation between $\mathbf{r}'$ and $\mathbf{r}$. In general this makes the interpretation of scattering experiments more complicated and we shall examine under what limits this expression may be reduced to the simpler expressions conventionally used. However, the conditions for this turn out to be more stringent for x rays than for visible light. For highly coherent beams, $R(\mathbf{r}',\mathbf{r})$ contains slit diffraction effects and $\varrho_F(\mathbf{r})$ contains finite sample diffraction effects that may yield highly oscillating forms for $I(\mathbf{q})$.

We proceed in the next section to evaluate $I(\mathbf{q})$ in the general case of a partially coherent incident beam, with finite slits and detector apertures and finite distances to and from the sample.

II. HUYGENS-FRESNEL THEORY FOR SCATTERING OF PARTIALLY COHERENT RADIATION

We consider the setup illustrated schematically in Fig. 1, where the beam emerges from an aperture A (slit), the plane of which is normal to the mean direction of the beam and the line joining its center to the sample center a distance L_1 away, and is then transmitted through an aperture B normally oriented to the average direction of the scattered beam at a distance L_2 from the center of the sample S, and finally counted in a detector D behind aperture B. According to the standard Huygens-Fresnel principle,[15] the statistical properties of the electric field at the aperture B and the intensity in the detector D can now be completely specified by knowing the spatial and temporal behavior of the electric field across aperture A, and the electron density in the sample. We neglect for the moment time-dependent effects and assume that $\varrho(\mathbf{r})$ is a static function. The resultant scattering will be affected by both coherence and resolution effects, in the sense discussed in Sec. I, but in general in a more complicated way. Let us consider each polarization component of the light separately, and let it be described in terms of a complex (analytic) signal given by

$$U_\alpha(\mathbf{s},t) = A_\alpha(\mathbf{s},t) \exp(-i\overline{\omega}t), \tag{13}$$

where $U_\alpha(\mathbf{s},t)$ represents the analytical field for polarization α at position s in the aperture A (measured relative to the center of A), $\overline{\omega}$ is the average frequency of the radiation, and the time dependence of the amplitude $A_\alpha(\mathbf{s},t)$ represents the relatively slow variation (on time scales much larger than $1/\overline{\omega}$) due to the nonmonochromaticity of the beam. We may define a mutual coherence function (MCF) for the radiation of polarization α

$$\Gamma_\alpha(\mathbf{s},\mathbf{s}',\tau) = \langle A_\alpha(\mathbf{s},t) A_\alpha^*(\mathbf{s}',t+\tau) \rangle, \tag{14}$$

where the average represents a time average on t over many phase fluctuations of the radiation (typically the latter have a time scale 10^{-15}–10^{-16} seconds for x rays). We may write[15,17–19]

$$\Gamma_\alpha(\mathbf{s},\mathbf{s}',\tau) = \Psi(\mathbf{s}) \Psi^*(\mathbf{s}') g(\mathbf{s}-\mathbf{s}') F(\tau) (I_\alpha/A), \tag{15}$$

as a rather general form for the MCF, where I_α is the total beam intensity through the aperture area A. We shall for simplicity neglect here the possible dependence of coherence lengths and times on the polarization of the radiation, although such explicit dependence may be easily incorporated in the formalism below, by letting $\Psi(\mathbf{s})$, $g(\mathbf{s}-\mathbf{s}')$, and $F(\tau)$ explicitly depend on the suffix α. The form chosen for the MCF in Eq. (15) is not the most general possible form, but is commonly used and is known as the generalized Schell form.[19,20] The function $\Psi(\mathbf{s})$ is called the amplitude factor, and $g(\mathbf{s}-\mathbf{s}')$ is called the coherence factor. The latter is defined to be unity when $\mathbf{s}=\mathbf{s}'$. The intensity of radiation at the position $\mathbf{s}$ in the slit is given by setting $\mathbf{s}=\mathbf{s}'$, and $\tau=0$ in Eq. (15), i.e., it is $\Psi(\mathbf{s})\Psi^*(\mathbf{s})$. It should be borne in mind that a uniform intensity does not necessarily imply that $\Psi(\mathbf{s})=1$, since one may have a pure phase field where $\Psi(\mathbf{s})=\exp\{i\phi(\mathbf{s})\}$. The form of Eq. (15) can also arise from a superposition of a set of mutually *incoherent* waves, each described by $\Psi(\mathbf{s})$, with an angular distribution of propagation vectors given by the Fourier transform of the function $g(\mathbf{x})$. If these are plane waves, then $\Psi(\mathbf{s})=1$, but in general $\Psi(\mathbf{s})$ can be used to represent curved wave fronts. It will be convenient to include the aperture cutoff function in our definition of $\Psi(\mathbf{s})$. The exact form of $\Psi(\mathbf{s})$ and $g(\mathbf{x})$ will depend on the nature and distance of the source of radiation from this aperture, and the optical elements in the beam prior to the slit (mirrors, monochromators, etc.) and can be difficult to calculate. We thus regard the form of the MCF across the incident aperture as empirical, ultimately obtainable from experiment. However, we introduce here the concept of coherence lengths which are implicitly contained in the MCF. If $g(\mathbf{x})$ is approximated by a Gaussian form, i.e.,

$$g(\mathbf{x})=\exp\left(-\frac{1}{2}\,x^2/\xi_x^2\right)\exp\left(-\frac{1}{2}\,y^2/\xi_y^2\right), \tag{16}$$

then ξ_x,ξ_y can be considered as the two *transverse coherence lengths*. The time autocorrelation function $F(\tau)$ decays with a characteristic time τ_l and we may define a *longitudinal coherence length* $\xi_l=c\tau_l$, c being the speed of light. In fact we shall note here that since $\Gamma_\alpha(\mathbf{s},\mathbf{s}',\tau)$ has to fulfill Helmholz equations in $\mathbf{s}$ and $\mathbf{s}'$ the ansatz given by Eq. (15) restricts the time autocorrelation function $F(\tau)$ to a pure exponential[15,19]

$$F(\tau)=F_0\exp(-\tau/\tau_l), \tag{17}$$

where we have to set $F_0=1$ by definition. We now proceed to the calculation of the MCF at the ''outgoing beam'' aperture B. In passing we note that this provides in principle a method for calculating how the coherence properties of the beam are affected by scattering from the sample (which may itself be an optical element in the beam). Finally, the scattered count rate is obtained by integrating the intensity of the scattered field at any point on the detector D over the detector area, since field amplitudes at different points on the detector cannot interfere. Here we would like to emphasize that the final result of our calculations does *not* necessarily have to obey the reciprocity theorem in the sense of a symmetry with respect to an exchange of the incident aperture A and the detector. The reason for this is that we have on the one hand a (partially) coherent ''source'' (aperture A) fully described by its MCF and on the other hand an incoherent detector. In this sense the detector is optically the reciprocal of a completely incoherent source.

We assume in the following that L_1 and L_2 are much larger than the typical aperture dimensions of A and B. Using the Huygens-Fresnel principle, and assuming kinematic scattering (i.e., no multiple scattering from the sample), the amplitude at time t arriving at the point $\mathbf{u}$ on the aperture B (measured relative to its center), after being scattered from a small volume element d$\mathbf{r}$ at a point $\mathbf{r}$ (relative to the sample center) and originating from an element $d\mathbf{s}$ of area around the point $\mathbf{s}$ in the aperture A (measured relative to the center of A), tracing the path $PP'P''$ in Fig. 1 is given by (for polarization α)

$$V_\alpha(\mathbf{u},t)=M_\alpha\left(\frac{e^2}{mc^2}\right)\frac{i}{\lambda}\,\varrho(\mathbf{r})d\mathbf{r}\,A_\alpha\left(\mathbf{s},t-\frac{P'P''+PP'}{c}\right)\times\frac{1}{PP'}\,\frac{1}{P'P''}\exp\left\{-i\overline{\omega}\left(t-\frac{P'P''+PP'}{c}\right)\right\}d\mathbf{s}, \tag{18}$$

where M_α is a polarization factor, and we have set the usual obliquity factor $\chi(\Theta)\approx 1$, where Θ is the angle between the actual path considered and the mean path for the incident or scattered beams, since $\Theta\ll 1$. Similarly the amplitude at $\mathbf{u}'$ arising from a different path $QQ'Q''$ in Fig. 1 is given by a similar expression with PP', $P'P''$ replaced by QQ', $Q'Q''$, respectively. Since two orthogonal polarizations are always incoherent[15,19] we may obtain independent MCF's for each polarization, yielding for the MCF at the aperture B

$$\begin{aligned}\Gamma_\alpha(\mathbf{u},\mathbf{u}',\tau)&=\langle V_\alpha(\mathbf{u},t)V_\alpha^*(\mathbf{u}',t+\tau)\rangle\\&=M_\alpha^2\left(\frac{e^2}{mc^2}\right)^2\frac{1}{\lambda^2}\int\int d\mathbf{r}\,d\mathbf{r}'\int\int d\mathbf{s}\,d\mathbf{s}'\varrho(\mathbf{r})\\&\quad\times\varrho(\mathbf{r}')\left\langle A_\alpha\left(\mathbf{s},t-\frac{P'P''+PP'}{c}\right)A_\alpha^*\left(\mathbf{s}',t+\tau\right.\right.\\&\quad\left.\left.-\frac{Q'Q''+QQ'}{c}\right)\right\rangle\exp\left\{i\,\frac{\overline{\omega}}{c}\,(P'P''-Q'Q''\right.\\&\quad\left.+PP'-QQ')\right\}\exp(i\overline{\omega\tau})\\&\quad\times\frac{1}{PP'}\,\frac{1}{P'P''}\,\frac{1}{QQ'}\,\frac{1}{Q'Q''},\end{aligned} \tag{19}$$

where $\langle\cdots\rangle$ denotes an average over t, i.e., over many phase fluctuations of the incident radiation. Let $\alpha=1$ define the polarization direction normal to the plane of scattering (i.e., the plane containing $OO'O''$ in Fig. 1). Then $M_1^2=1$. The other polarization ($\alpha=2$) has $M_2^2=\cos(2\vartheta_s)$, where ϑ_s is the average scattering angle. The integrals over $\mathbf{s},\mathbf{s}'$ are two-dimensional (2D) integrals over the slit aperture A, and over $\mathbf{r},\mathbf{r}'$ are 3D integrals over the sample volume. In this average, making an appropriate translation in time coordinates and defining a path difference

$$\Delta l=P'P''-Q'Q''+PP'-QQ', \tag{20}$$

and using Eq. (14), we may write

$$\Gamma_\alpha(\mathbf{u},\mathbf{u}',\tau)=M_\alpha^2\left(\frac{e^2}{mc^2}\right)^2\frac{1}{\lambda^2}\int\int d\mathbf{r}\,d\mathbf{r}'\int\int d\mathbf{s}\,d\mathbf{s}'\varrho(\mathbf{r})\times\varrho(\mathbf{r}')\Gamma_\alpha(\mathbf{s},\mathbf{s}',\tau+\Delta l/c)\exp(i\overline{\omega}\Delta l/c)\times\exp(i\overline{\omega}\tau)\,\frac{1}{PP'}\,\frac{1}{P'P''}\,\frac{1}{QQ'}\,\frac{1}{Q'Q''}. \tag{21}$$

To second order in $\mathbf{s},\mathbf{s}',\mathbf{u},\mathbf{u}',\mathbf{r},\mathbf{r}'$ it may be verified easily that

$$\Delta l=(\mathbf{r}'-\mathbf{r})\cdot(\hat{\mathbf{k}}_2-\hat{\mathbf{k}}_1)+\frac{1}{2L_1}[(\mathbf{r}-\mathbf{s})^2-(\mathbf{r}'-\mathbf{s}')^2+(\mathbf{r}'\cdot\hat{\mathbf{k}}_1)^2-(\mathbf{r}\cdot\hat{\mathbf{k}}_1)^2]+\frac{1}{2L_2}[(\mathbf{r}-\mathbf{u})^2-(\mathbf{r}'-\mathbf{u}')^2+(\mathbf{r}'\cdot\hat{\mathbf{k}}_2)^2-(\mathbf{r}\cdot\hat{\mathbf{k}}_2)^2], \tag{22}$$

where $\hat{\mathbf{k}}_1$ and $\hat{\mathbf{k}}_2$ are unit vectors along OO' and $O'O''$, respectively. Since $\overline{\omega/c}=k_0$, the magnitude of the mean incident wave vector, and $k_0(\hat{\mathbf{k}}_2-\hat{\mathbf{k}}_1)=\mathbf{q}$, the nominal wave vector transfer, we may write

$$\frac{\overline{\omega}}{c}\Delta l=\mathbf{q}\cdot(\mathbf{r}'-\mathbf{r})+\frac{k_{L_1}^2}{2}[\mathbf{s}^2-\mathbf{s}'^2-2\mathbf{r}\cdot\mathbf{s}+2\mathbf{r}'\cdot\mathbf{s}'+\mathbf{r}_{\perp,1}^2-\mathbf{r}_{\perp,1}'^2]+\frac{k_{L_2}^2}{2}[\mathbf{u}^2-\mathbf{u}'^2-2\mathbf{r}\cdot\mathbf{u}+2\mathbf{r}'\cdot\mathbf{u}'+\mathbf{r}_{\perp,2}^2-\mathbf{r}_{\perp,2}'^2], \tag{23}$$

where we have defined

$$k_{L_1}=\sqrt{k_0/L_1},\quad\text{and}\quad k_{L_2}=\sqrt{k_0/L_2}, \tag{24}$$

for notational convenience and $\mathbf{r}_{\perp,1}$ and $\mathbf{r}_{\perp,2}$ are the components of $\mathbf{r}$ perpendicular to $\hat{\mathbf{k}}_1$ and $\hat{\mathbf{k}}_2$, respectively, and similarly for $\mathbf{r}'$.

In the denominators of Eq. (21), we may replace PP', $P'P''$, etc., by L_1, L_2, etc. If $\Gamma_\alpha(\mathbf{s},\mathbf{s}',\tau)$ given by Eq. (15) is introduced and $F(\tau)$ is replaced by its Fourier integral

$$F(\tau)=\frac{1}{2\pi}\int d\Delta\omega\,\tilde{F}(\Delta\omega)\exp(-i\Delta\omega\tau), \tag{25}$$

we obtain

$$\Gamma_\alpha(\mathbf{u},\mathbf{u}',\tau)=M_\alpha^2\left(\frac{e^2}{mc^2}\right)^2\frac{1}{2\pi\lambda^2}\frac{1}{L_1^2}\frac{1}{L_2^2}\frac{I_\alpha}{A}\int\int d\mathbf{s}\,d\mathbf{s}'\times\int\int d\mathbf{r}\,d\mathbf{r}'\int d\Delta\omega\,\Psi(\mathbf{s})\Psi^*(\mathbf{s}')g(\mathbf{s}-\mathbf{s}')\times\tilde{F}(\Delta\omega)\exp\{i(\overline{\omega}-\Delta\omega)\tau\}\times\exp\{i(\overline{\omega}-\Delta\omega)\Delta l/c\}\varrho(\mathbf{r})\varrho(\mathbf{r}'). \tag{26}$$

Let us write this as

$$\Gamma_\alpha(\mathbf{u},\mathbf{u}',\tau)=M_\alpha^2\left(\frac{e^2}{mc^2}\right)^2\frac{\overline{\omega}}{2\pi\lambda^2}\frac{1}{L_1^2}\frac{1}{L_2^2}\frac{I_\alpha}{A}\Gamma'(\mathbf{u},\mathbf{u}',\tau), \tag{27}$$

with

$$\Gamma'(\mathbf{u},\mathbf{u}',\tau)=\int d\Omega\;\tilde{F}[\overline{\omega}(1-\Omega)]\exp(i\overline{\omega}\Omega\tau)\int\int d\mathbf{s}\,d\mathbf{s}'\Psi(\mathbf{s})\Psi^*(\mathbf{s}')g(\mathbf{s}-\mathbf{s}')\int\int d\mathbf{r}\,d\mathbf{r}'\exp\{-i\Omega(\mathbf{q}+k_{L_1}^2\mathbf{s}+k_{L_2}^2\mathbf{u})\cdot\mathbf{r}\}\times\exp\{i\Omega(\mathbf{q}+K_{L_1}^2\mathbf{s}'+k_{L_2}^2\mathbf{u}')\cdot\mathbf{r}'\}\exp\left\{i\,\frac{\Omega}{2}\,k_{L_1}^2(s^2-s'^2)\right\}\exp\left\{i\,\frac{\Omega}{2}\,k_{L_2}^2(u^2-u'^2)\right\}\times\varrho(\mathbf{r})\exp\left\{i\,\frac{\Omega}{2}\,(k_{L_1}^2\mathbf{r}_{\perp,1}^2+k_{L_2}^2\mathbf{r}_{\perp,2}^2)\right\}\varrho(\mathbf{r}')\exp\left\{-i\,\frac{\Omega}{2}\,(k_{L_1}^2\mathbf{r}_{\perp,1}'^2+k_{L_2}^2\mathbf{r}_{\perp,2}'^2)\right\}, \tag{28}$$

where we have used Eq. (23) and the definition

$$\Omega=1-\Delta\omega/\overline{\omega}=1+\Delta\lambda/\lambda. \tag{29}$$

Here $\Delta\lambda/\lambda$ is the deviation from the monochromaticity of the incoming radiation. If we now make the definition of a modified density $\varrho_F(\mathbf{r})$, throughout this paper referred to as the *Fresnel electron density*, by

$$\varrho_F(\mathbf{r})=\varrho(\mathbf{r})\exp\left\{i\,\frac{\Omega}{2}\,(k_{L_1}^2\mathbf{r}_{\perp,1}^2+k_{L_2}^2\mathbf{r}_{\perp,2}^2)\right\}, \tag{30}$$

we note that the $\mathbf{r}$ and $\mathbf{r}'$ integrations in Eq. (28) may be carried out yielding the Fourier transform of ϱ_F and ϱ_F^*, respectively (see Sec. II B).

A. Real space discussion

The Eqs. (27) and (28) represent the central result of our paper. The only conditions that must pertain for this result to be valid are (a) the kinematic approximation for scattering and (b) the distances L_1, L_2 must be much larger than the aperture and sample dimensions.

It should be noted that the result given by Eq. (28) is still symmetric with respect to the quantities $\mathbf{s}$, $\mathbf{s}'$ and $\mathbf{u},\mathbf{u}'$. Since $\Gamma'(\mathbf{u},\mathbf{u}',\tau)$ describes how the MCF of aperture A propagates to the sample and then to aperture B, an exchange of A and B does not affect the net result thus satisfying the reciprocity theorem.

If a detector is placed behind the outgoing aperture and detects *all* the radiation passing through, the measured intensity will be given by

$$I(\mathbf{q})=\sum_{\alpha}\int_{B}d\mathbf{u}\langle|V_{\alpha}(\mathbf{u},t)|^{2}\rangle \tag{31}$$

$$=\sum_{\alpha}\int_{B}d\mathbf{u}\;\Gamma_{\alpha}(\mathbf{u},\mathbf{u},\tau=0) \tag{32}$$

$$=\sum_{\alpha}M_{\alpha}^{2}\left(\frac{e^{2}}{mc^{2}}\right)^{2}\frac{\overline{\omega}}{2\pi\lambda^{2}}\frac{1}{L_{1}^{2}}\frac{1}{L_{2}^{2}}\frac{I_{\alpha}}{A}\times\int_{B}d\mathbf{u}\;\Gamma'(\mathbf{u},\mathbf{u},0), \tag{33}$$

where the integral is taken over aperture B and we have used Eq. (27). We now examine the form of $\int d\mathbf{u}\;\Gamma'(\mathbf{u},\mathbf{u},0)$. Let us replace the variable of integration Ω in Eq. (28) by the magnitude of the vector $\mathbf{Q}$, where

$$\mathbf{Q}=\Omega\mathbf{q}, \tag{34}$$

and we obtain

$$S(\mathbf{q})=\int_{B}d\mathbf{u}\;\Gamma'(\mathbf{u},\mathbf{u},0)=\frac{q}{k_{L_2}^{4}}\int\frac{dQ}{Q^{2}}\widetilde{F}[(q-Q)\overline{\omega/q}]\times\int_{S}d\mathbf{u}'\hat{S}_{Q}(\mathbf{Q}+\mathbf{u}'), \tag{35}$$

where $\mathbf{u}'=(Q/q)k_{L_2}^{2}\mathbf{u}$ and the integral over $d\mathbf{u}'$ is over the outgoing aperture dimensions scaled by $(Q/q)k_{L_2}^{2}$, and

$$\hat{S}_{Q}(\mathbf{K})=\int\int d\mathbf{r}\;d\mathbf{r}'\varrho_{F}(\mathbf{r})\varrho_{F}^{*}(\mathbf{r}')R_{Q}(\mathbf{r}',\mathbf{r})\times\exp\{i\mathbf{K}\cdot(\mathbf{r}'-\mathbf{r})\}, \tag{36}$$

where

$$R_{Q}(\mathbf{r}',\mathbf{r})=\int\int d\mathbf{s}\;d\mathbf{s}'\Psi(\mathbf{s})\Psi^{*}(\mathbf{s}')g(\mathbf{s}-\mathbf{s}')\times\exp\left\{i\frac{Q}{2q}k_{L_1}^{2}(s^{2}-s'^{2})\right\}\times\exp\left\{i\frac{Q}{q}k_{L_1}^{2}(\mathbf{s}'\cdot\mathbf{r}'-\mathbf{s}\cdot\mathbf{r})\right\}. \tag{37}$$

In Eqs. (36) and (37) we have used the subscript Q on the functions $\hat{S}_{Q}(\mathbf{K})$ and $R_{Q}(\mathbf{r}',\mathbf{r})$ to indicate an additional parametric dependence on the magnitude of $\mathbf{Q}$. By Eq. (17), we have

$$\widetilde{F}[(q-Q)\overline{\omega/q}]=\frac{\xi_{l}/c}{1+(k_{0}\xi_{l}/q)^{2}(q-Q)^{2}}, \tag{38}$$

where we have defined the longitudinal coherence length $\xi_{l}=c\tau_{l}$. Equation (35) then becomes

$$S(\mathbf{q})=\frac{q\xi_{l}}{k_{L_2}^{4}c}\int\frac{dQ}{Q^{2}}\frac{1}{1+(k_{0}\xi_{l}/q)^{2}(q-Q)^{2}}\times\int_{S}d\mathbf{u}'\hat{S}_{Q}(\mathbf{Q}+\mathbf{u}'). \tag{39}$$

Equation (39) has a simple interpretation. It is the function $\hat{S}_{Q}(\mathbf{K})$ folded with the resolution over the outgoing detector slits, and the resultant function which depends parametrically on Q folded with the Lorentzian resolution function (for the longitudinal coherence) centered at q. This would be identical to the conventional formalism if $\hat{S}_{Q}(\mathbf{K})$ were the conventional function $S_{0}(\mathbf{K})$ folded with the angular resolution of the incident beam. However, $\hat{S}_{Q}(\mathbf{K})$ defined by Eq. (36) has a slightly more complicated form; namely, $\varrho(\mathbf{r})$ is replaced by the Fresnel density $\varrho_{F}(\mathbf{r})$ and $R_{Q}(\mathbf{r}',\mathbf{r})$ is not simply a function of $(\mathbf{r}'-\mathbf{r})$ as in Eq. (7). We note furthermore from Eq. (39) that the *effective* longitudinal coherence length for a particular experiment is ξ_{l} multiplied by the factor (k_{0}/q), thus magnifying this quantity considerably for experiments where q is small (e.g., surface scattering experiments). The fact that one can work with fairly small longitudinal coherence lengths in this regime is already well known.[6,14]

From now on for notational convenience, we shall omit the suffix Q at $\hat{S}_{Q}(\mathbf{K})$ and $R_{Q}(\mathbf{r}',\mathbf{r})$ and we always replace (Q/q) again by the variable Ω as introduced before [see Eqs. (29) and (34)]. We note that $\Omega=1$ $(Q=q)$ means $\Delta\lambda/\lambda=0$, i.e., the case of a perfectly monochromatic beam.

We may also express $\hat{S}(\mathbf{K})$ directly in terms of the usual electron density-density correlation function by inserting the explicit form of the Fresnel density from Eq. (30) into Eq. (36) and we get

$$\hat{S}(\mathbf{K})=\int\int d\mathbf{r}\;d\mathbf{r}'\varrho(\mathbf{r})\varrho(\mathbf{r}')R_{1}(\mathbf{r}',\mathbf{r})\exp\{i\mathbf{K}\cdot(\mathbf{r}'-\mathbf{r})\}, \tag{40}$$

where

$$R_{1}(\mathbf{r}',\mathbf{r})=\Gamma_{s}(\mathbf{r}',\mathbf{r},0)\exp\left\{i\frac{\Omega}{2}k_{L_2}^{2}(\mathbf{r}_{\perp,2}^{2}-\mathbf{r}_{\perp,2}'^{2})\right\}, \tag{41}$$

and

$$\Gamma_{s}(\mathbf{r}',\mathbf{r},0)=\int\int d\mathbf{s}\;d\mathbf{s}'\Psi(\mathbf{s})\Psi^{*}(\mathbf{s}')g(\mathbf{s}-\mathbf{s}')\times\exp\left\{i\frac{\Omega}{2}k_{L_1}^{2}[(\mathbf{s}-\mathbf{r}_{\perp,1})^{2}-(\mathbf{s}'-\mathbf{r}'_{\perp,1})^{2}]\right\}. \tag{42}$$

We note that $\Gamma_{s}(\mathbf{r}',\mathbf{r},0)$ defined by Eq. (42) is nothing else but the transverse MCF of the incident radiation from aperture A *at the sample position*, apart from the usual longitudinal propagation phase factor $\exp\{-i\mathbf{k}_{1}\cdot(\mathbf{r}'-\mathbf{r})\}$, as may be verified by an analogous calculation to that in Eqs. (18)–(28). It is the spatial range of this MCF which determines the range of spatial separation of points in the sample which can produce interference, i.e., the coherence volume, and it is tempting to parametrize this MCF as a function of $(\mathbf{r}-\mathbf{r}')_{\perp}$ as in Eq. (16) thus avoiding the calculation of Eq. (42). However, we note that from Eq. (42) this function cannot in general be written simply as a function of $(\mathbf{r}'-\mathbf{r})$, except in the so-called ''incoherent limit'' of aperture A to be discussed below. Moreover, we believe that our formula-

tion in terms of the MCF across the incident aperture A maintains the symmetry between incident and scattered radiation and is to be preferred.

The properties of the transverse MCF $\Gamma_s(\mathbf{r}',\mathbf{r},0)$ determine what is seen in a scattering experiment, after integration over the detector aperture and a radial integration over the wave vector transfer with a ''longitudinal resolution function'' which is a Lorentzian of width $q/(k_0\xi_l)$. An expression for $\Gamma_s(\mathbf{r}',\mathbf{r},0)$, based on a Gaussian approximation, is given in Appendix B.

Assuming an isotropic transverse coherence length ξ_t across aperture A, the transverse coherence length *at the sample* ξ_s and the transverse beam size *at the sample* w are given by

$$\xi_s=\left[\xi_t^2\left(1+\frac{1}{k_{L_1}^4\sigma^4}\right)+\frac{2}{k_{L_1}^4\sigma^2}\right]^{1/2} \tag{43}$$

and

$$w=\sigma\frac{\xi_s}{\xi_t}, \tag{44}$$

where σ is the lateral dimension of aperture A (assumed the same in the x and y directions). Thus, if $\xi_t\ll\sigma$, there are many coherence volumes inside the illuminated sample volume and we are in the incoherent limit, regardless of the distance L_1, unless ξ_s becomes larger than the actual dimension of the sample l, in which case the beam is coherent across the entire sample. In the case that $(\xi_s/l)\sim 1$ ''speckle'' will be observed for a disordered sample provided the lateral size of each detector element w_d satisfies $w_d<\lambda L_2/(2l)$ and the distance a between structural elements in the scatterer satisfies $a<(2\pi/q)(\pi\xi_l/\lambda)$.

The coherence lengths can also be used to estimate the range of separation between two points in the sample from which the scattering can interfere. If these points are separated by a distance $\Delta\mathbf{r}$, then the condition is that (Δr) must be less than either $(\xi_s/\sin\alpha)$ (where α is the angle between $\Delta\mathbf{r}$ and the incident beam direction) or $(k_0\xi_l/q_0)$, where q_0 is the component of $\mathbf{q}$ along $\Delta\mathbf{r}$. We may now discuss under what conditions $I(\mathbf{q})$ takes the form of the conventional expression as given by Eqs. (6) or (7), or where the more general expression must be used.

In the *coherent limit*, $\xi_t\gg\sigma$, and we may replace $g(\mathbf{s}-\mathbf{s}')$ by unity so that Eqs. (41) and (42) yield

$$R_1(\mathbf{r}',\mathbf{r})=T^*(\mathbf{r}')T(\mathbf{r}), \tag{45}$$

where

$$T(\mathbf{r})=\exp\left\{i\frac{\Omega}{2}(k_{L_1}^2\mathbf{r}_{\perp,1}^2+k_{L_2}^2\mathbf{r}_{\perp,2}^2)\right\}\int d\mathbf{s}\;\Psi(\mathbf{s})$$
$$\times\exp\left(i\frac{\Omega}{2}k_{L_1}^2s^2\right)\exp(-i\Omega k_{L_1}^2\mathbf{s}\cdot\mathbf{r}). \tag{46}$$

Thus $\hat{S}(\mathbf{K})$ is the Fourier transform of the correlation function $[\varrho_{\rm eff}(\mathbf{r})\varrho_{\rm eff}^*(\mathbf{r}')]$ where

$$\varrho_{\rm eff}(\mathbf{r})=\varrho(\mathbf{r})T(\mathbf{r}). \tag{47}$$

The function $T(\mathbf{r})$ incorporates incident aperture diffraction effects. If

$$L_1,L_2\gg l^2/\lambda\quad(w>l) \tag{48}$$

or

$$L_1,L_2\gg w^2/\lambda\quad(w<l), \tag{49}$$

then we may neglect the Fresnel factor in the diffraction from the sample. If in addition

$$L_1\gg\sigma^2/\lambda, \tag{50}$$

then $T(\mathbf{r})\simeq 1$ and $\varrho_{\rm eff}(\mathbf{r})\simeq\varrho(\mathbf{r})$. We term this the *Fraunhofer limit*. It would appear that for x rays, this limit can only be satisfied for very large values of L_1,L_2. However, if the sample is not itself coherent (e.g., made up of microcrystallites), l may be taken for some purposes as the grain size. In any case, if $l>w$, by Eq. (49) it is the *beam size at the sample* and not the sample size which determines the condition for the Fraunhofer regime.

Also in this limit $\xi_s=\xi_t$, unless σ is very small or L_1 is very large, so that $w\simeq\sigma$. Thus, for a 10 μm crystallite or beam size at a wavelength of $\lambda=1$ Å, the Fraunhofer regime is attained if $L_1,L_2\gg 1$ m.

In the *incoherent limit* $(\xi_t\ll\sigma)$, by Eq. (43)

$$\xi_s=\frac{1}{\sqrt{2}\pi}\frac{\lambda L_1}{\sigma}. \tag{51}$$

If in addition, we assume that

$$\xi_t\ll\xi_s \tag{52}$$

then, setting $\Omega\simeq 1$ in Eq. (37) (i.e., neglecting longitudinal effects) we can neglect the Fresnel factor in Eq. (37) across aperture A, and obtain

$$R_Q(\mathbf{r}',\mathbf{r})\approx\int d\mathbf{s}|\Psi(\mathbf{s})|^2\exp\{i\Omega k_{L_1}^2\mathbf{s}\cdot(\mathbf{r}'-\mathbf{r})\}, \tag{53}$$

which looks similar to the form of Eq. (7) provided $\varrho(\mathbf{r})$ is replaced by the *Fresnel density* $\varrho_F(\mathbf{r})$. To consider when we may neglect this difference, let us consider again the effective size l of a coherently scattering region in a direction transverse to the beam. We need to consider two cases:

(a) $l>\xi_s$. In this case, the Fresnel factor for the incident beam can be neglected if

$$k_{L_1}^2 l\xi_s\ll 2\pi, \tag{54}$$

which by Eq. (51) reduces to

$$l/\sigma\ll 1. \tag{55}$$

For the scattered beam, the corresponding condition is

$$k_{L_2}^2 l\xi_s\ll 2\pi \tag{56}$$

or, thus,

$$l/\sigma\ll L_2/L_1. \tag{57}$$

Inequalities (55) and (57) are the conditions for the Fraunhofer regime to be attained in this case. The reason that Eq.

(55) is independent of L_1 is that the decrease in $k_{L_1}^2$ is exactly cancelled by the increase in ξ_s as L_1 increases.

(b) $l<\xi_s$ (this will happen if L_1 becomes large enough). In this case the Fraunhofer regime is attained when

$$k_{L_1}^2 l^2, k_{L_2}^2 l^2 \ll 2\pi, \tag{58}$$

which reduces to

$$L_1, L_2 \gg l^2/\lambda, \tag{59}$$

conditions which are similar to the coherent case.

B. Reciprocal space treatment

It is often preferable to evaluate the expressions for the scattered intensities in reciprocal rather than real space. By Fourier transforming Eq. (36) we may write $\hat{S}(\mathbf{K})$ in the reciprocal space form

$$\hat{S}(\mathbf{K}) = \int\int d\mathbf{s}\, d\mathbf{s}' \Psi(\mathbf{s})\Psi^*(\mathbf{s}') g(\mathbf{s}-\mathbf{s}') \exp\left\{ i\,\frac{\Omega}{2}\, k_{L_1}^2 (s^2 - s'^2) \right\} \widetilde{\varrho}_F(\mathbf{K}+\Omega k_{L_1}^2 \mathbf{s}) \widetilde{\varrho}_F^*(\mathbf{K}+\Omega k_{L_1}^2 \mathbf{s}'). \tag{60}$$

The arguments of the Fourier transform of the Fresnel density $\widetilde{\varrho}_F(\mathbf{K})$ represent the Cartesian components (K_x, K_y, K_z) relative to the (x,y,z) axes shown in Fig. 1, where the z axis is along the average incident beam direction. In scattering experiments often sample-fixed coordinates are more appropriate and a back transformation of the components has to be performed (see Sec. V).

Again, in the (true) incoherent limit, this reduces to

$$\hat{S}(\mathbf{K}) = \int d\mathbf{s} |\Psi(\mathbf{s})|^2 |\widetilde{\varrho}_F(\mathbf{K}+\Omega k_{L_1}^2 \mathbf{s})|^2, \tag{61}$$

i.e., $|\widetilde{\varrho}_F(\mathbf{K})|^2$ folded with the incident aperture resolution function, as discussed above. In this case no incident slit diffraction effects are expected, while in the coherent limit we get

$$\hat{S}(\mathbf{K}) = \left| \int d\mathbf{s}\ \Psi(\mathbf{s}) \exp(i\Omega k_{L_1}^2 s^2/2) \widetilde{\varrho}_F(\mathbf{K}+\Omega k_{L_1}^2 \mathbf{s}) \right|^2, \tag{62}$$

i.e., $\widetilde{\varrho}_F(\mathbf{K})$ *first* folded with the incident aperture resolution (including Fresnel diffraction effects) and then modulus squared. As we shall see, this can result in interference between different diffraction peaks which overlap in reciprocal space resulting in a complex diffraction pattern.

We may also manipulate Eq. (60) into a related form which may be convenient for calculations. If we define a function

$$T(\mathbf{s},\mathbf{K}) = \Psi(\mathbf{s}) \exp(i\Omega k_{L_1}^2 s^2/2) \widetilde{\varrho}_F(\mathbf{K}+\Omega k_{L_1}^2 \mathbf{s}), \tag{63}$$

and its 2D Fourier transform with respect to $\mathbf{s}$ by $\widetilde{T}(\mathbf{P},\mathbf{K})$, and similarly that of $g(\mathbf{s})$ by $\widetilde{g}(\mathbf{P})$ then Eq. (60) may be written as

$$\hat{S}(\mathbf{K}) = \int\int d\mathbf{s}\, d\mathbf{s}' T(\mathbf{s},\mathbf{K}) g(\mathbf{s}-\mathbf{s}') T^*(\mathbf{s}',\mathbf{K}) = 4\pi^2 \int d\mathbf{P} |\widetilde{T}(\mathbf{P},\mathbf{K})|^2 \widetilde{g}(\mathbf{P}). \tag{64}$$

Consider the case where $\varrho(\mathbf{r})$ represents a thin screen with apertures in it (in the beam direction), such that $\varrho(\mathbf{r})=0$ in the opaque regions and $\varrho(\mathbf{r})=1$ in the aperture regions [$\mathbf{r}$ being confined to the (x,y) plane only, so $\widetilde{\varrho}(q_x,q_y,q_z)$ becomes independent of q_z]. Then Eq. (64) reduces to the formulas given by Nugent[17] and others[8] for diffraction by partially coherent radiation apart from the fact that Eq. (63) contains the Fourier transform of the Fresnel density $\varrho_F(\mathbf{r})$ rather than that of the real (Fraunhofer) electron density $\varrho(\mathbf{r})$. For most applications we can take $\Psi(\mathbf{s})$ simply to be the aperture function (1 inside the aperture, 0 outside) and assume a simple (e.g., Gaussian) functional form for $g(\mathbf{s}-\mathbf{s}')$ in terms of which we can define our transverse coherence lengths quantitatively [see Eq. (16)].

We shall now use these results to calculate the form of the scattering for several simple cases under various conditions.

III. FRESNEL DENSITY

The fact, that the scattered intensity is related to the Fourier transform of the Fresnel electron density $\widetilde{\varrho}_F(\mathbf{K})$ rather than being simply related to the Fourier transform of the actual density, except in the Fraunhofer regime discussed above, is the main difference between our final result given by Eq. (60) and the common treatment. Since

$$\varrho_F(\mathbf{r}) = \varrho(\mathbf{r}) \exp\left\{ i\,\frac{\Omega}{2}\,(k_{L_1}^2 \mathbf{r}_{\perp,1}^2 + k_{L_2}^2 \mathbf{r}_{\perp,2}^2) \right\}, \tag{65}$$

the Fresnel density depends on the monochromaticity and direction of the incoming and scattered x rays. Therefore $\varrho_F(\mathbf{r})$ is *not* an electron density in the common sense and we will now express $\widetilde{\varrho}_F(\mathbf{K})$ in terms of the Fourier transform of the real density $\widetilde{\varrho}(\mathbf{K})$ and a $\mathbf{K}$-space function $\widetilde{\mathcal{F}}(\mathbf{K})$ which is unique for all further calculations. From Eq. (65) follows

$$\widetilde{\varrho}_F(\mathbf{K}) = \widetilde{\varrho}(\mathbf{K}) * \widetilde{\mathcal{F}}(\mathbf{K}), \tag{66}$$

where the asterisk again denotes a convolution and $\widetilde{\mathcal{F}}(\mathbf{K})$ is given by

$$\widetilde{\mathcal{F}}(\mathbf{K}) = \int d\mathbf{r}\ \exp(-i\mathbf{K}\cdot\mathbf{r}) \exp\left\{ i\,\frac{\Omega}{2}\,(k_{L_1}^2 \mathbf{r}_{\perp,1}^2 + k_{L_2}^2 \mathbf{r}_{\perp,2}^2) \right\}. \tag{67}$$

For reasons of simplicity we restrict ourselves throughout this paper to the case of in-plane scattering. Then the directions $\hat{\mathbf{k}}_1$ and $\hat{\mathbf{k}}_2$ are given in laboratory fixed coordinates with the z axis along the mean direction of the incoming beam (see Fig. 1) by

$$\hat{\mathbf{k}}_1 = (0,0,1), \tag{68}$$

$$\hat{\mathbf{k}}_2 = (0, \sin\Phi, \cos\Phi), \tag{69}$$

where Φ denotes the angle between the mean directions of the incident and scattered radiation (often also called 2θ). After a straightforward calculation the integral given by Eq. (67) yields

$$\tilde{\mathcal{F}}(\mathbf{K}) = C(\Omega,\Phi)\exp\left\{-\frac{i}{2\Omega}\frac{K_x^2}{k_{L_1}^2+k_{L_2}^2}\right\}\exp\left\{-\frac{i}{2\Omega}\left[\frac{K_{yz}^2}{k_{L_1}^2} + \frac{K_z^2}{k_{L_2}^2\sin^2\Phi}\right]\right\}, \tag{70}$$

where the prefactor is given by

$$C(\Omega,\Phi) = \frac{2(i-1)}{k_{L_1}k_{L_2}(k_{L_1}^2+k_{L_2}^2)^{1/2}}\left(\frac{\pi}{\Omega}\right)^{3/2}\frac{1}{\sin\Phi}, \tag{71}$$

and the definition

$$K_{yz} = K_y + K_z\cot\Phi \tag{72}$$

was used. In the following the subscript yz always means that the y and z components of the respective vector (here $\mathbf{K}$) have to be combined in the manner given by Eq. (72). With the explicit representation of the delta function

$$\delta(x) = \lim_{\epsilon\to 0}\frac{1+i}{\sqrt{2\pi\epsilon}}\exp(-ix^2/\epsilon^2), \tag{73}$$

it is easy to prove that in the limit $k_{L_1},k_{L_2}\to 0$ (i.e., $L_1,L_2\to\infty$)

$$\tilde{\mathcal{F}}(\mathbf{K})\to(2\pi)^3\delta(\mathbf{K}) \tag{74}$$

holds, and we regain the usual result $\tilde{\varrho}_F(\mathbf{K}) = \tilde{\varrho}(\mathbf{K})$. In the next sections we calculate the scattering for particular cases (Bragg reflections, surfaces) using the result given by Eq. (60) and the expressions given by Eqs. (66) and (70).

IV. BRAGG REFLECTIONS

An interesting feature of Eq. (60) in the partially coherent case is that *different* Fourier components of the electron density can interfere in reciprocal space if they are close enough to overlap within the broadening due to the incident slit. Consider for example diffraction from a perfect infinite crystal in the kinematic limit. We have

$$\tilde{\varrho}_\infty(\mathbf{K}) = V_a^{-1}\sum_{\mathbf{G}}\tilde{\varrho}(\mathbf{G})\,\delta(\mathbf{K}-\mathbf{G}), \tag{75}$$

where $\mathbf{G}$ represent the reciprocal vectors of the crystal lattice and V_a is the volume of the unit cell. For a single isolated Bragg-reflection this would lead to an apparent paradox, since by Eqs. (66) and (70), $|\tilde{\varrho}_F(\mathbf{K})|^2$ would be *independent* of $(\mathbf{K}-\mathbf{G})$ resulting in no peak in the scattering. However, an infinite crystal violates our assumptions of the sample dimensions being much smaller than L_1,L_2. A real crystal is finite with dimensions $l_x,l_y,l_z \ll L_1,L_2$. Alternatively the beam size at the crystal is finite. We denote by l the smaller of the two lengths in what follows, and we always use the term ''sample size'' bearing in mind that this may be only the smaller beam size, too. The Fourier transform of the actual electron density $\tilde{\varrho}(\mathbf{K})$ may be written as

$$\tilde{\varrho}(\mathbf{K}) = \tilde{\varrho}_\infty(\mathbf{K}) * \tilde{\mathcal{T}}(\mathbf{K}), \tag{76}$$

with a reciprocal space truncation function[21,22]

$$\tilde{\mathcal{T}}(\mathbf{K}) = \int_{l_x,l_y,l_z} d\mathbf{r}\,\exp(i\mathbf{K}\cdot\mathbf{r}). \tag{77}$$

The shape of the crystal enters into the resultant formulas via the borders of the (x,y,z) integral. If a sharp cut rectangular crystal is assumed this would lead to oscillatory Fresnel integrals in the final expression for $\tilde{\varrho}_F(\mathbf{K})$. However, it is more realistic to assume that the sample edges are smoothed out and do not give rise to additional oscillations. Therefore we choose a Gaussian in real space,

$$\mathcal{T}(\mathbf{r}) = \exp(-r^2\pi^2/l^2), \tag{78}$$

with the corresponding Fourier transform

$$\tilde{\mathcal{T}}(\mathbf{K}) = (2\pi\Delta^2)^{-3/2}\exp(-K^2/\Delta^2), \tag{79}$$

as the truncation function, where we assumed for simplicity $l_x = l_y = l_z = l$, i.e., that the sample is isotropic, and $\Delta = 2\pi/l$. Note that this is the 3D equivalent of the famous Warren approximation for finite 2D crystals.[23]

Then the Fresnel density may be calculated by a double convolution from the density $\tilde{\varrho}_\infty(\mathbf{K})$ of an infinite periodic crystal given by Eq. (75):

$$\tilde{\varrho}_F(\mathbf{K}) = \tilde{\varrho}_\infty(\mathbf{K}) * \tilde{\mathcal{T}}(\mathbf{K}) * \tilde{\mathcal{F}}(\mathbf{K}). \tag{80}$$

Alternatively we may calculate $\tilde{\varrho}_F(\mathbf{K})$ by a single Fourier transform after a complete real space treatment. This way is explicitly shown in Appendix A. Finally, we obtain the result

$$\tilde{\varrho}_F(\mathbf{K}) = C_1(\Omega,\Phi)V_a^{-1}\sum_{\mathbf{G}}\tilde{\varrho}(\mathbf{G}) \times\exp\left\{-\frac{i}{2\Omega}\frac{1-i\epsilon_x^2}{1+\epsilon_x^4}\frac{(\delta K_x)^2}{k_{L_1}^2+k_{L_2}^2}\right\} \times\exp\left\{-\frac{i}{2\Omega k_{L_1}^2}\frac{\sum_{n=0}^{3} f_n(\delta\mathbf{K})\epsilon^{2n}}{\sum_{m=0}^{2} g_m\epsilon^{4m}}\right\}. \tag{81}$$

The quantities ϵ_x and ϵ are defined by

$$\epsilon = \left(\frac{1}{2\Omega}\right)^{1/2}\frac{\Delta}{k_{L_1}},$$

and

$$\epsilon_x = \left(\frac{1}{2\Omega}\right)^{1/2}\frac{\Delta}{(k_{L_1}^2+k_{L_2}^2)^{1/2}}, \tag{82}$$

and the prefactor $C_1(\Omega,\Phi)$ is given by

$$C_1(\Omega,\Phi)=\frac{C(\Omega,\Phi)}{(1+i\epsilon_x^2)^{1/2}[1+i(\chi+\sin^{-2}\Phi)\epsilon^2-\chi\epsilon^4]^{1/2}}, \tag{83}$$

where we introduced

$$\chi=\frac{k_{L_1}^2}{k_{L_2}^2}\frac{1}{\sin^2\Phi} \tag{84}$$

for notational convenience. Note that in the case of a large crystal, $\Delta\to 0$, we have $C_1(\Omega,\Phi)\to C(\Omega,\Phi)$. The $f_n(\delta\mathbf{K})$ and g_m terms in the second exponential are

$$f_0(\delta\mathbf{K})=(\delta K_{yz})^2+\chi(\delta K_z)^2, \tag{85}$$

$$f_1(\delta\mathbf{K})=-i\{(\delta K_{yz})^2+(\chi\delta K_z+\delta K_{yz}\cot\Phi)^2\}, \tag{86}$$

$$f_2(\delta\mathbf{K})=\chi\{\chi(\delta K_y)^2+(\delta K_z-\delta K_y\cot\Phi)^2\}, \tag{87}$$

$$f_3(\delta\mathbf{K})=-i\chi^2\{(\delta K_y)^2+(\delta K_z)^2\}, \tag{88}$$

$$g_0=1, \tag{89}$$

$$g_1=(\chi+\sin^{-2}\Phi)^2-2\chi, \tag{90}$$

$$g_2=\chi^2. \tag{91}$$

Here $\delta\mathbf{K}=\mathbf{K}-\mathbf{G}$ denotes the deviation of $\mathbf{K}$ from a reciprocal lattice point $\mathbf{G}$, and δK_{yz} is given in terms of the components δK_y and δK_z according to Eq. (72).

Equation (81) is the exact result for the Fresnel density in the case of Bragg reflections from finite crystals. From what has been said previously, we do not need to discuss explicitly the Fraunhofer limit which would simply yield $\hat{S}(\mathbf{K})$ proportional to the Fourier transform of the electron density because then we have $\epsilon,\epsilon_x\gg 1$ (i.e., $lk_{L_{1,2}}\ll 2\pi$), and Eq. (81) reduces to (only the $n=2,3$ and $m=2$ terms are kept)

$$\tilde{\varrho}_F(\mathbf{K})=\frac{l^3}{(2\pi)^{3/2}V_a}\sum_{\mathbf{G}}\tilde{\varrho}(\mathbf{G})\exp\left\{-\frac{l^2(\delta K)^2}{4\pi^2}\right\}, \tag{92}$$

which is the usual $\tilde{\varrho}(\mathbf{K})$ of a *finite* crystal.

Another approximation is to take the *extreme Fresnel limit* defined by

$$k_{L_{1,2}}^2 w^2\gg 2\pi$$

or

$$\epsilon,\epsilon_x\ll 1. \tag{93}$$

Since most scattering experiments deal with wavelengths of $\lambda\sim 1$ Å, distances $L_1,L_2\sim 1$ m, and sample sizes of $l\sim 1$ mm we get (with $\Omega\sim 1$)

$$\epsilon,\epsilon_x\sim\left(\frac{\pi}{\Omega}\frac{\lambda L_{1,2}}{l^2}\right)^{1/2}\approx 0.02\ll 1, \tag{94}$$

and this approximation is well satisfied. Keeping only terms up to ϵ^2, ϵ_x^2 in the exponentials and inserting $\tilde{\varrho}_F(\mathbf{K})$ into Eq. (60) yields the result $[C_1(\Omega,\Phi)\approx C(\Omega,\Phi)]$

$$\begin{aligned}\hat{S}(\mathbf{K})=V_a^{-2}\sum_{\mathbf{G},\mathbf{G}'}&\tilde{\varrho}(\mathbf{G})\tilde{\varrho}^*(\mathbf{G}')\tilde{\mathcal{F}}(\delta\mathbf{K})\tilde{\mathcal{F}}^*(\delta\mathbf{K}')\\&\times\int\int d\mathbf{s}\,d\mathbf{s}'\Psi(\mathbf{s})\Psi^*(\mathbf{s}')g(\mathbf{s}-\mathbf{s}')\\&\times\exp\left\{i\frac{\Omega}{2}\frac{k_{L_1}^2k_{L_2}^2}{k_{L_1}^2+k_{L_2}^2}(s_x^2-s_x'^2)\right\}\\&\times\exp\left\{i\frac{k_{L_1}^2}{k_{L_1}^2+k_{L_2}^2}(\delta K_x's_x'-\delta K_xs_x)\right\}\\&\times\exp\{i(\delta K_{yz}'s_y'-\delta K_{yz}s_y)\}\tilde{\mathcal{P}}[(\delta\mathbf{K}/\Omega)+k_{L_1}^2s]\\&\times\tilde{\mathcal{P}}[(\delta\mathbf{K}'/\Omega)+k_{L_1}^2\mathbf{s}'],\end{aligned} \tag{95}$$

where $\tilde{\mathcal{F}}(\mathbf{K})$ is given by Eq. (70). In Eq. (95) the following notation is used:

$$\delta\mathbf{K}=\mathbf{K}-\mathbf{G}=(\delta K_x,\delta K_y,\delta K_z), \tag{96}$$

$$\delta\mathbf{K}'=\mathbf{K}-\mathbf{G}'=(\delta K_x',\delta K_y',\delta K_z'), \tag{97}$$

$$\delta K_{yz}=\delta K_y+\delta K_z\cot\Phi, \tag{98}$$

$$\delta K_{yz}'=\delta K_y'+\delta K_z'\cot\Phi. \tag{99}$$

The function $\tilde{\mathcal{P}}[K_x,K_y,K_z]$ defines the shape of the Bragg reflections in reciprocal space which is caused by the finite size of the sample. It is given by

$$\begin{aligned}\tilde{\mathcal{P}}[K_x,K_y,K_z]=\exp\left\{-\frac{1}{4}\frac{K_x^2\Delta^2}{(k_{L_1}^2+k_{L_2}^2)^2}\right\}\exp\Bigg\{-\frac{1}{4}\frac{\Delta^2}{k_{L_1}^4}[K_{yz}^2\\+(K_{yz}\cot\Phi+\chi(\Phi)K_z)^2]\Bigg\}.\end{aligned} \tag{100}$$

We get as a result a series of Gaussians $\tilde{\mathcal{P}}[K_x,K_y,K_z]$ in reciprocal space of width $\sim lk_{L_{1,2}}^2/\pi$ which have to be folded with the detector and longitudinal resolution according to Eq. (39). We may neglect $\mathbf{G}\neq\mathbf{G}'$ terms if $|\mathbf{G}-\mathbf{G}'|>\pi^{-1}(l^2+s_0^2)^{1/2}k_{L_{1,2}}^2$ where s_0 denotes the slit width. It is interesting to note that in this limit, i.e., in the limit of $\epsilon,\epsilon_x\ll 1$, the width of the peaks in reciprocal space gets *smaller* with l. However, as $l\to 0$ we violate the condition $\epsilon,\epsilon_x\ll 1$ for the extreme Fresnel case and pass to the Fraunhofer limit given by Eq. (92) where we see that the widths of the peaks *increase* as l gets smaller which is the more familiar situation.

We will now explicitly discuss the incoherent and coherent limits of Eq. (95) in the next two subsections.

A. Incoherent limit

In the incoherent limit $g(\mathbf{s}-\mathbf{s}')$ is only appreciable for $\mathbf{s}\approx\mathbf{s}'$, i.e., ξ_x, ξ_y are much smaller than all aperture dimensions.[24] If the limit $\mathbf{G}\approx\mathbf{G}'$ is assumed in Eq. (95) and new variables $\mathbf{s}^-=\mathbf{s}-\mathbf{s}'$ and $\mathbf{s}^+=\mathbf{s}+\mathbf{s}'$ are introduced, the two $\mathbf{s}$, $\mathbf{s}'$ integrations can be separated, and one may easily verify the result

$$\hat{S}(\mathbf{K}) \approx V_a^{-2} \sum_{\mathbf{G}} |\tilde{\varrho}(\mathbf{G})|^2 \tilde{g}\left[\frac{k_{L_1}^2}{k_{L_1}^2+k_{L_2}^2}\,\delta K_x, \delta K_{yz}\right] \times \frac{1}{k_{L_1}^4}\left|\Psi\left[\frac{1}{\Omega k_{L_1}^2}\,(\delta K_x, \delta K_y)\right]\right|^2 \times (\tilde{\mathcal{P}}[\delta\mathbf{K}/\Omega])^2, \tag{101}$$

where $\tilde{g}(K_x, K_{yz})$ denotes the Fourier transform with respect to s_x, s_y of the coherence factor $g(\mathbf{s})$ and $\Psi(\mathbf{s})$ is the *real* space aperture function as explained in Sec. II. Thus in the incoherent limit we regain the result of single Bragg reflections with intensity proportional to $|\tilde{\varrho}(\mathbf{G})|^2$. The shape of the peaks is determined by three factors: (i) The Fourier transform of the coherence function $g(\mathbf{s})$. This has a width in reciprocal space which is $\sim 1/\xi_t$, where ξ_t is a typical transverse coherence length at the incident aperture. (ii) The real space function $\Psi(\mathbf{s})$ yielding the direct shape of the aperture as shape of the respective Bragg reflections. This has a width in $\delta\mathbf{K}$ which is $\sim 1/\xi_s$, where ξ_s is given by Eq. (43). (iii) The reciprocal space function $\tilde{\mathcal{P}}[K_x, K_y, K_z]$ which takes the finite size of the sample into account. This also has a width in $\delta\mathbf{K}$ which is $\sim 1/\xi_s$ if the sample and slit sizes are comparable. Note that if $\xi_t \ll \xi_s$ the function $\tilde{g}(K_x, K_{yz})$ may be replaced by a constant in Eq. (101) yielding the incoherent limit as discussed in Sec. II A.

B. Coherent limit

The other interesting limit is that of a highly spatial coherent beam ($\xi_x, \xi_y \to \infty$) impinging on the first aperture A and being Bragg reflected by a single crystal. Then we have $g(\mathbf{s}-\mathbf{s}') \approx 1$ and Eq. (95) may be completely separated in $\mathbf{s}$, $\mathbf{s}'$ and $\delta\mathbf{K}, \delta\mathbf{K}'$. Thus we obtain

$$\hat{S}(\mathbf{K}) = \left| V_a^{-1} \sum_{\mathbf{G}} \tilde{\varrho}(\mathbf{G}) \tilde{\mathcal{F}}(\delta\mathbf{K})\, \frac{1}{k_{L_1}^4}\, \tilde{\Psi}_F\left[\frac{k_{L_1}^2}{k_{L_1}^2+k_{L_2}^2}\,\delta K_x, \delta K_{yz}\right] \mathcal{P}_F\left[\frac{\delta K_x}{k_{L_1}^2+k_{L_2}^2}, \frac{\delta K_{yz}}{k_{L_1}^2}, \frac{\delta K_z}{\Omega}\right]\right|^2, \tag{102}$$

where $\mathcal{P}_F[\delta K_x, \delta K_y, \delta K_z]$ is the 2D Fourier transform with respect to (x,y) of the function

$$\mathcal{P}_F[x, y, \delta K_z] = \mathcal{P}[x, y, \delta K_z] \exp\left\{\frac{i}{\Omega}\,[(k_{L_1}^2+k_{L_2}^2)x^2 + k_{L_1}^2 y^2]\right\}, \tag{103}$$

with $\mathcal{P}[x, y, \delta K_z]$ the 2D Fourier transform with respect to the first two variables of the peak function $\tilde{\mathcal{P}}[K_x, K_y, K_z]$ defined in Eq. (100). Furthermore $\tilde{\Psi}_F(K_x, K_{yz})$ represents the Fourier transform of

$$\Psi_F(\mathbf{s}) = \Psi(\mathbf{s}) \exp\left\{ i\, \frac{\Omega}{2}\, \frac{k_{L_1}^2 k_{L_2}^2}{k_{L_1}^2+k_{L_2}^2}\, s_x^2 \right\}, \tag{104}$$

i.e., $\tilde{\Psi}_F(K_x, K_{yz})$ is the Fourier transform of the aperture function $\Psi(\mathbf{s})$ decorated by Fresnel terms in the out of plane direction x. We would like to emphasize the surprising fact that the Fresnel terms in the scattering plane exactly cancel in our calculations, i.e., *no* quadratic s_y terms occur in Eq. (102). Although the final result looks similar to a first order approximation in s_y, i.e., similar to the Fraunhofer case, the result that every Bragg reflection is decorated by the Fourier transform of the aperture function is a direct consequence of keeping all *second* order terms (Fresnel limit) throughout the calculations of Sec. II.

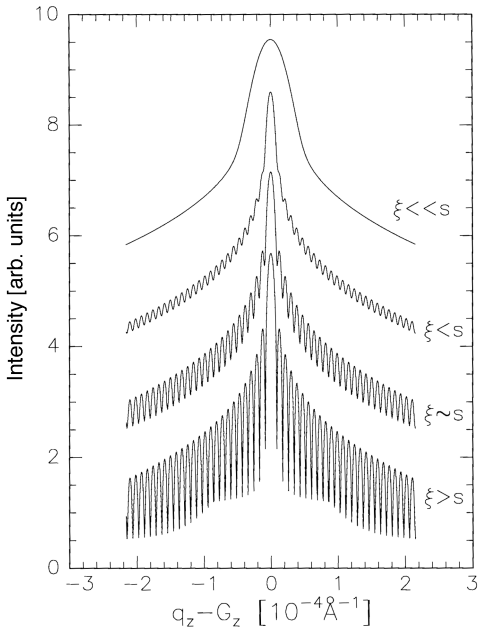

FIG. 2. Intensity around a symmetric Bragg reflection at $\mathbf{G} = (0,0,G_z)$ for different coherence lengths ξ in the extreme Fresnel case. The intensity is calculated along the vertical direction $q_{z'}$. The slit width was $s = 50\ \mu$m and from the bottom to the top ξ decreases ($\xi > s$ coherent limit, $\xi \sim s$, $\xi < s$ intermediate cases, $\xi \ll s$ incoherent limit).

C. Examples

We will now present examples for the abovementioned results for Bragg reflections. All calculations were performed using Eqs. (60) and (81). The successive foldings with the detector resolution and the longitudinal coherence according to Eq. (39) were not taken into account (i.e., we set $\mathbf{K} = \mathbf{q}$ and $\Omega = 1$). Furthermore we do not consider the out-of-plane direction, i.e., we always assume $K_x = G_x = 0$. As aperture A we assume a rectangular slit with width s in the y direction. The parameters which are the same for all calculations are the x-ray wavelength $\lambda = 1$ Å, the slit width $s = 50\ \mu$m, the location of the Brag reflection $\mathbf{G}' = (0,0,G_{z'})$ and $G_{z'} = 2.18$ Å^{-1}, and the sample size $l = 1$ mm. We always assume symmetric configuration, i.e., we take $L_1 = L_2$.

Figures 2 and 3 show the intensity distribution around a Bragg reflection for different in-plane coherence lengths $\xi_t = \xi_y = \xi$ along $q_{z'}$ and $q_{y'}$, respectively. The sample-incident–exit aperture distance was $L_{1,2} = 1$ m yielding $\epsilon = 0.02 \ll 1$ (extreme Fresnel limit). From the top to the bottom we have $\xi = 5\ \mu\text{m} \ll s$ (incoherent limit but *not* the true

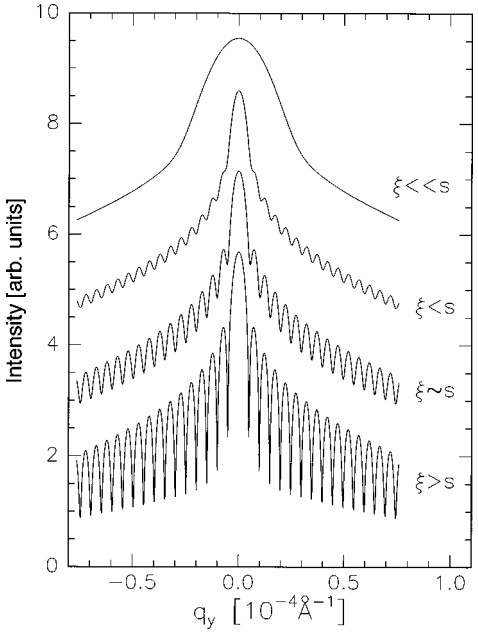

FIG. 3. Intensity around a symmetric Bragg reflection at $\mathbf{G}=(0,0,G_z)$ for different coherence lengths ξ in the extreme Fresnel case. The intensity is calculated along the transverse direction $q_{y'}$. The slit width was $s=50\ \mu$m and from the bottom to the top ξ decreases ($\xi>s$ coherent limit, $\xi\sim s$, $\xi<s$ intermediate cases, $\xi\ll s$ incoherent limit).

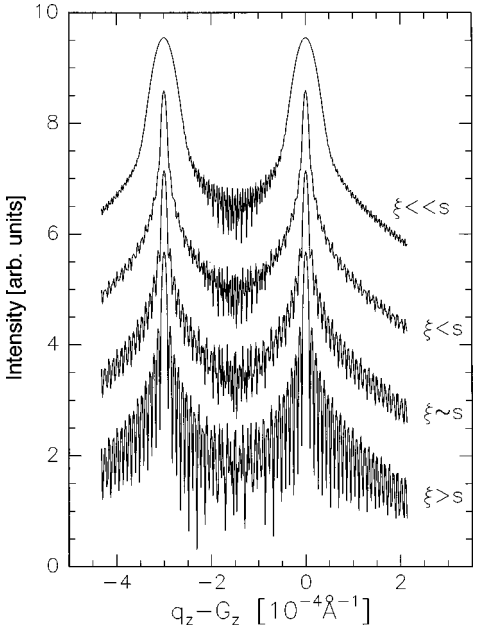

FIG. 4. Interference of two Bragg reflections as function of the transverse coherence length ξ in the extreme Fresnel case. The slit width was $s=50\ \mu$m and from the bottom to the top ξ decreases ($\xi>s$ coherent limit, $\xi\sim s$, $\xi<s$ intermediate cases, $\xi\ll s$ incoherent limit). Note that the peaks do not overlap.

incoherent limit in the sense that ξ_t is not $\ll\xi_s=2\ \mu$m), $\xi=25\ \mu\text{m}<s$, $\xi=50\ \mu\text{m}\sim s$, and $\xi=100\ \mu\text{m}>s$ (coherent limit). One can see that in the incoherent limit we have a broad peak with width $1/\xi_t\approx 2\times 10^{-5}$ Å^{-1} as already shown analytically in Sec. IV A, whereas the peak is considerably more narrow when the coherence length is of the order of the aperture width. Then the Bragg reflection is decorated with the Fourier transform of the incident aperture with most pronounced modulations in the coherent limit.

Figures 4 and 5 demonstrate interference effects which may occur if two Bragg reflections are close together in reciprocal space. The same parameter values as for Figs. 2 and 3 were used and we chose the same structure factors $\tilde{\varrho}(\mathbf{G})$ for both reflections. In Fig. 4 even weak interferences are visible in the incoherent limit because we are in the extreme Fresnel regime. These interferences become more and more pronounced with increasing coherence length ξ. In Fig. 5 we have calculated the intensity along $q_{z'}$ in the coherent limit $\xi\gg s$ as a function of the distance between both reflections. One can see that the closer the peaks are, the more pronounced the interference effects become.

Figures 6 and 7 show the Bragg reflection in the coherent and incoherent limits as a function of the sample-incident–exit aperture distance $L_{1,2}$. We note that for very large distances the oscillations from the aperture disappear and both the coherent and incoherent limit yield the same result (Fraunhofer limit). This is more clearly demonstrated in Fig. 8 where the full width at half maximum (FWHM) of a Bragg reflection as function of $L_{1,2}$ is plotted. It can be seen that the FWHM remains constant in most of the extreme Fresnel regime ($\epsilon\ll 1$). In the incoherent (but *not* true incoherent $\xi_t\ll\xi_s$) limit (open triangles) this value is $1/\xi_t$ (see Sec. IV A) and in the coherent limit (open circles) this constant value is $2\pi/s$. From a certain length $L_{1,2}$ the width of the Gaussian given by $\tilde{\mathcal{P}}(\delta\mathbf{K})$ in Eq. (95) is smaller than that constant value and the FWHM decreases linearly with increasing $L_{1,2}$.

In the Fresnel ($\epsilon\sim 1$) and Fraunhofer ($\epsilon\gg 1$) regimes the same FWHM is obtained regardless of whether we take the coherent or incoherent limit. This is a direct consequence of the fact that even an incoherent beam exhibits a certain degree of coherence by the time the radiation reaches the

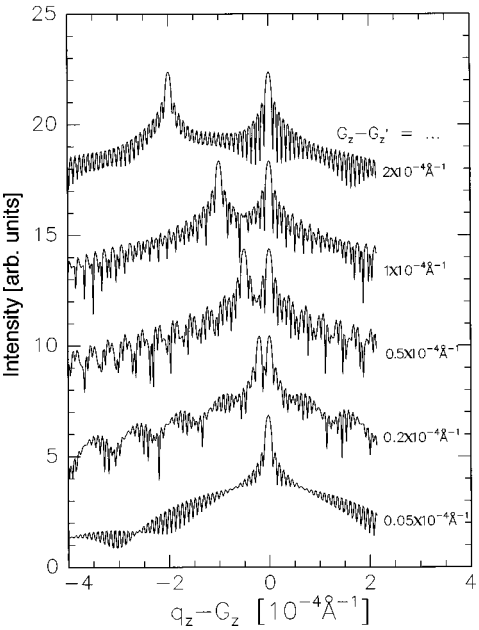

FIG. 5. Interference of two symmetrical Bragg reflections as function of their distance G_z-G_z' in reciprocal space in the extreme Fresnel case and for the coherent limit $\xi\gg s$.

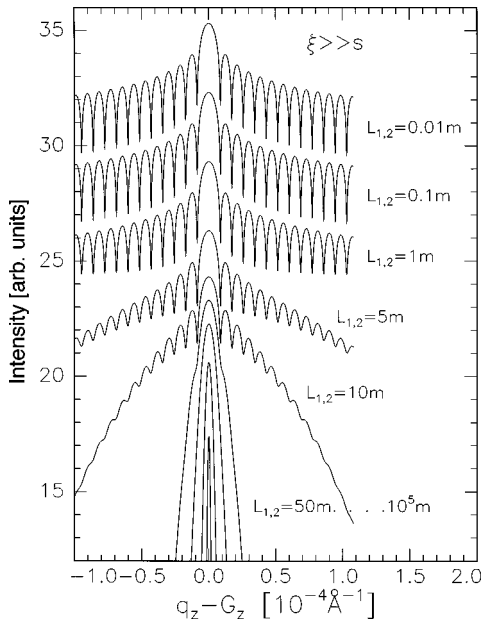

FIG. 6. Bragg reflection at $q_z = G_z$ for different incident/exit aperture-sample distance $L_{1,2}$ in the coherent limit (coherence length $\xi \gg s$ slit width). The curves shown are mainly in the extreme Fresnel regime $0.01\ \mathrm{m} \leqslant L_{1,2} \leqslant 100\ \mathrm{m}$ and the Fraunhofer region $L_{1,2} \geqslant 10^4$ m.

sample (see discussion in Sec. II A). For very large distances $L_{1,2}$ the FWHM remains constant at the value $2\pi/l$ (Fraunhofer case).

We note from Fig. 8 that a usual scattering experiment always is performed in the extreme Fresnel limit and *not* as often anticipated in the Fraunhofer regime, which starts for the realistic parameter values which we have assumed for the calculations, at distances $L_{1,2} > 10^4$ m. But we must repeat

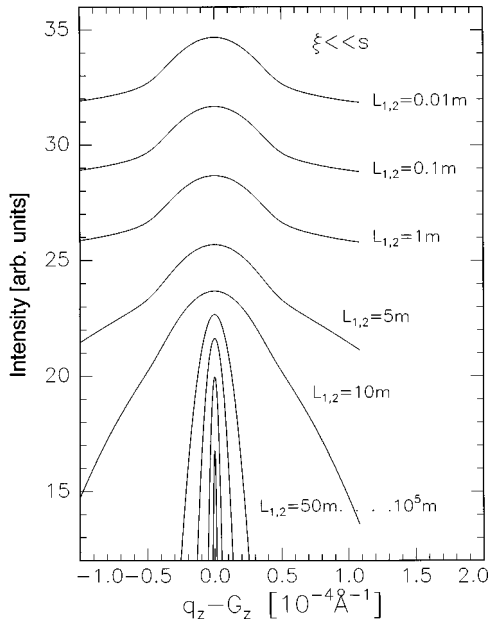

FIG. 7. Bragg reflection at $q_z = G_z$ for different incident/exit aperture-sample distance $L_{1,2}$ in the incoherent limit (coherence length $\xi \gg s$ slit width). The curves shown are mainly in the extreme Fresnel regime $0.01\ \mathrm{m} \leqslant L_{1,2} \leqslant 100\ \mathrm{m}$ and the Fraunhofer region $L_{1,2} \geqslant 10^4$ m.

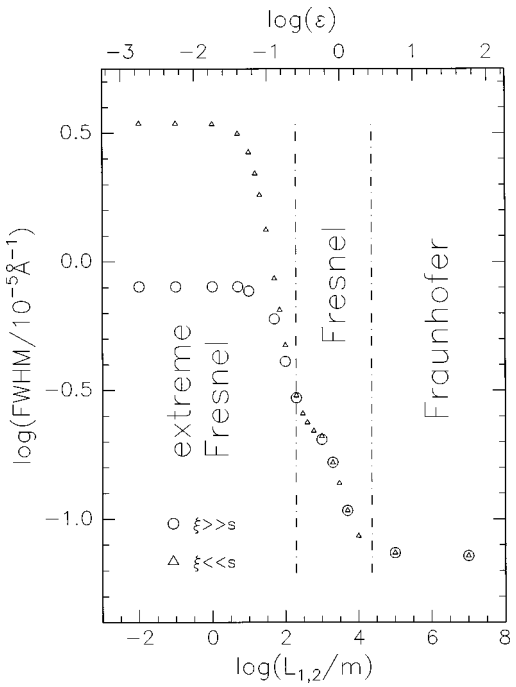

FIG. 8. Full width at half maximum (FWHM) of a Bragg reflection as function of the incident/exit aperture-sample distance $L_{1,2}$. The open circles are the values for the coherent limit ($\xi \gg s$) whereas the open triangles give the results for the incoherent limit ($\xi \ll s$). Note that both curves are almost identical in the Fresnel and Fraunhofer regimes, i.e., for $\epsilon > 0.3$.

that the examples in Figs. 2–8 do not include detector resolution, longitudinal coherence effects, and possible imperfections which may destroy the coherence at the sample position.

V. SURFACES

Specular and diffuse scattering from rough surfaces must also be considered carefully when partially coherent radiation is involved, since the usual ensemble averages over the height fluctuations cannot be made right away. We consider the geometry for one single rough surface making a grazing angle of incidence α to the incident beam. The exit angle is denoted by $\beta = \Phi - \alpha$ throughout this paragraph. We choose surface-fixed coordinates (x',y',z') such that x' is in the plane of the surface and parallel to the space fixed (incident slit) x axis and z' is normal to the average surface (see Fig. 1). Relative to the axes (x',y',z') the Fourier components of the ideal electron density $\tilde{\varrho}_\infty(\mathbf{K}')$ are[25]

$$\tilde{\varrho}_\infty(K_{x'},K_{y'},K_{z'}) = i\,\frac{\tilde{\varrho}_0}{K_{z'}} \int\int dx'dy' \times \exp\{-iK_{z'}h(x',y')\} \times \exp\{-i(K_{x'}x' + K_{y'}y')\}, \tag{105}$$

where $\tilde{\varrho}_0$ is the electron density of the medium under the surface, and $h(x',y')$ defines the surface contour. Here we note that the description given by Eq. (105) already includes

finite size effects in the z' direction (absorption). Therefore we only have to truncate $\varrho_\infty(\mathbf{r}')$ by a 2D Gaussian in the x' and y' directions:

$$\mathcal{T}_S(\mathbf{r}')=\exp\{-(x'^2+y'^2)\pi^2/l'^2\}, \tag{106}$$

in real space, with the Fourier transform

$$\widetilde{\mathcal{T}}_S(\mathbf{K}')=(\sqrt{2\pi}\Delta')^{-2}\exp\{-(K_{x'}^2+K_{y'}^2)/\Delta'^2\}\delta(K_{z'}), \tag{107}$$

where we again assumed for simplicity $l_x=l_y=l'$ and $\Delta'=2\pi/l'$. The Fresnel density then may be calculated similarly to the case of Bragg reflections via

$$\widetilde{\varrho}_F(\mathbf{K}')=\widetilde{\varrho}_\infty(\mathbf{K}')*\widetilde{\mathcal{T}}_S(\mathbf{K}')*\widetilde{\mathcal{F}}(\mathbf{K}'), \tag{108}$$

where we note that $\mathbf{K}'=(K_{x'},K_{y'},K_{z'})$ is given in *surface fixed* coordinates and $\widetilde{\mathcal{F}}(\mathbf{K}')$ is given by Eq. (70). The transformation between the components of $\mathbf{K}'$ and those of $\mathbf{K}$ in laboratory coordinates is given by

$$K_{x'}=K_x, \tag{109}$$

$$K_{y'}=-K_y\sin\alpha+K_z\cos\alpha, \tag{110}$$

$$K_{z'}=-K_y\cos\alpha-K_z\sin\alpha. \tag{111}$$

A. Periodic surfaces

Since we now deal with the case of coherent radiation we do not want to apply statistical averages to describe the surface $h(x',y')$ via correlation functions. Therefore we first calculate the case of a 2D strictly periodic surface, i.e., we assume

$$h(x'+d_{x'},y')=h(x',y'+d_{y'})=h(x',y'), \tag{112}$$

which may be regarded as a particular ''rough'' surface with a few enhanced Fourier coefficients.[26,27] The exact result for the Fresnel density in surface-fixed coordinates $(K_{x'},K_{y'},K_{z'})$ may then be calculated to be

$$\begin{aligned}\widetilde{\varrho}_F(\mathbf{K}')=\widetilde{\varrho}_0 C_2(\Omega,\Phi)\sum_{m_x,m_y}\widetilde{\mathcal{F}}(K_{x',m_x},K_{y',m_y},K_{z'})\\ \times\exp\left\{-\frac{\epsilon_x'^2}{2\Omega(k_{L_1}^2+k_{L_2}^2)}\frac{K_{x',m_x}^2}{1+i\epsilon_x'^2}\right\}\\ \times\exp\left\{-\frac{\epsilon'^2}{2\Omega k_{L_1}^2}\frac{(\chi_c K_{y',m_y}+\chi_{sc}K_{z'})^2}{1+i\chi_c\epsilon'^2}\right\}\\ \times(\mathrm{erf}[\gamma_0(K_{y'},K_{z'})]\delta_{m_x,0}\delta_{m_y,0}\\ +\widetilde{H}_{m_x,m_y}[K_{y'},K_{z'};h(x',y')]),\end{aligned} \tag{113}$$

where ϵ_x' and ϵ' are given by

$$\epsilon'=\left(\frac{1}{2\Omega}\right)^{1/2}\frac{\Delta'}{k_{L_1}},$$

and

$$\epsilon_x'=\left(\frac{1}{2\Omega}\right)^{1/2}\frac{\Delta'}{(k_{L_1}^2+k_{L_2}^2)^{1/2}}, \tag{114}$$

the function $\widetilde{\mathcal{F}}(\mathbf{K})$ is defined by Eq. (70); χ, χ_c, χ_s, and χ_{sc} are given by

$$\chi=\frac{1}{\sin^2\Phi}\frac{k_{L_1}^2}{k_{L_2}^2}, \tag{115}$$

$$\chi_c=\frac{1}{\sin^2\Phi}\left(\frac{k_{L_1}^2}{k_{L_2}^2}\cos^2\alpha+\cos^2\beta\right), \tag{116}$$

$$\chi_s=\frac{1}{\sin^2\Phi}\left(\frac{k_{L_1}^2}{k_{L_2}^2}\sin^2\alpha+\sin^2\beta\right), \tag{117}$$

$$\chi_{sc}=\frac{1}{\sin^2\Phi}\left(\frac{k_{L_1}^2}{k_{L_2}^2}\sin\alpha\cos\alpha-\sin\beta\cos\beta\right), \tag{118}$$

and $C_2(\Omega,\Phi)$ is defined via

$$C_2(\Omega,\Phi)=\frac{\pi/2}{(1+i\epsilon_x'^2)^{1/2}(1+i\chi_c\epsilon'^2)^{1/2}}. \tag{119}$$

Since we have assumed a periodic surface $h(x',y')$ with periodicities $d_{x'}$ and $d_{y'}$ we may define the reciprocal space quantities (m_x,m_y are integers)

$$q_{m_x}=m_x\frac{2\pi}{d_{x'}},$$

and

$$q_{m_y}=m_y\frac{2\pi}{d_{y'}}, \tag{120}$$

and $\mathbf{K}'$-vector components relative to q_{m_x}, q_{m_y}

$$K_{x',m_x}=K_{x'}-q_{m_x}, \tag{121}$$

$$K_{y',m_y}=K_{y'}-q_{m_y}. \tag{122}$$

The argument $\gamma_{m_y}(K_{y'},K_{z'})$ of the error function in Eq. (113) is given by

$$\begin{aligned}\gamma_{m_y}(K_{y'},K_{z'})=\left(-\frac{i}{2\Omega k_{L_1}^2}\right)^{1/2}\\ \times\frac{\chi_{sc}K_{y',m_y}+(\chi_s+i\chi\epsilon'^2)K_{z'}}{(1+i\chi_c\epsilon'^2)^{1/2}(\chi_s+i\chi\epsilon'^2)^{1/2}},\end{aligned} \tag{123}$$

and $\widetilde{H}_{m_x,m_y}[K_{y'},K_{z'};h(x',y')]$ are Fourier coefficients which are directly related to the height function $h(x',y')$. Their explicit expression is

$$\widetilde{H}_{m_x,m_y}[K_{y'},K_{z'};h(x',y')]$$

$$= \frac{1}{d_{x'}d_{y'}} \int_0^{d_{x'}} \int_0^{d_{y'}} dx'dy' \frac{2}{\sqrt{\pi}} \left(\int_{\gamma_{m_y}}^{\gamma_{m_y}+\hat{\gamma}h(x',y')} dt \times \exp(-t^2) \right) \exp\{-i(q_{m_x}x' + q_{m_y}y')\}, \quad (124)$$

with

$$\hat{\gamma} = -\left(\frac{-i\Omega k_{L_1}^2}{2} \frac{1+i\chi_c\epsilon'^2}{\chi_s + i\chi\epsilon'^2} \right)^{1/2}. \quad (125)$$

Equation (113) is the result for the Fresnel density of a periodic surface without any approximations. In general $|\gamma_{m_y}(K_{y'},K_{z'})| \sim K_{z'}/k_{L_1}$ is a very large quantity and the expansion

$$\mathrm{erf}(z) \approx 1 - \frac{1}{\sqrt{\pi}z} \exp(-z^2) \quad (126)$$

is always justified.[28] Then Eq. (113) may be reduced to

$$\begin{aligned} \tilde{\varrho}_F(\mathbf{K}') = {} & \tilde{\varrho}_0 C_2(\Omega,\Phi) \tilde{\mathcal{F}}(\mathbf{K}') \tilde{\mathcal{P}}_1(\mathbf{K}'/\Omega) \delta_{m_{x'},0}\delta_{m_{y'},0} \\ & + i\tilde{\varrho}_0 (1+i\epsilon_x'^2)^{-1/2} (\overline{\chi}\chi_x/\chi_{sc})^{1/2} \\ & \times \sum_{m_x,m_y} \tilde{\mathcal{F}}_S(K_{x',m_x},K_{y',m_y}) \\ & \times \exp\left\{ -\frac{\epsilon_x'^2}{2\Omega(k_{L_1}^2+k_{L_2}^2)} \frac{K_{x',m_x}^2}{1+i\epsilon_x'^2} \right\} \\ & \times \exp\left\{ -\frac{\epsilon'^2}{2\Omega k_{L_1}^2} \frac{\chi^2\overline{\chi}K_{y',m_y}^2}{\chi_s\chi_{sc}} \right\} \\ & \times \frac{\tilde{h}_{m_x,m_y}^{(e)}(K_{y',m_y}\overline{\chi} + K_{z'})}{K_{y',m_y}\overline{\chi} + K_{z'}}, \end{aligned} \quad (127)$$

where we neglected terms of the order $[k_{L_{1,2}}h(x',y')]^2$ against $K_{z'}h(x',y')$ in the exponentials and terms of the order $k_{L_{1,2}}^2 h(x',y')$ against $K_{y'},K_{z'}$ in the denominator. Since $k_{L_{1,2}}^2 \sim 10^{-10}$ Å^{-2} (for $\lambda = 1$ Å and $L_{1,2} = 1$ m) in the x-ray regime this approximation is always well satisfied. Furthermore we introduced

$$\overline{\chi} = \frac{\chi_{sc}}{\chi_s + i\chi\epsilon'^2}, \quad (128)$$

for notational convenience, and

$$\begin{aligned} \tilde{h}_{m_x,m_y}^{(e)}(K_{z'}) = {} & \frac{1}{d_{x'}d_{y'}} \int_0^{d_{x'}} \int_0^{d_{y'}} dx'dy' \\ & \times \exp\{-iK_{z'}h(x',y')\} \exp\{-i(q_{m_x}x' \\ & + q_{m_y}y')\}. \end{aligned} \quad (129)$$

The function $\tilde{\mathcal{F}}_S(K_{x'},K_{y'})$ is given by

$$\tilde{\mathcal{F}}_S(K_{x'},K_{y'}) = C_S(\Omega,\Phi) \exp\left\{ -\frac{iK_{x'}^2}{2\Omega(k_{L_1}^2+k_{L_2}^2)} \right\} \times \exp\left\{ -\frac{iK_{y'}^2}{2\Omega k_{L_1}^2} \frac{\chi}{\chi_s} \right\}, \quad (130)$$

with

$$C_S(\Omega,\Phi) = \frac{2\pi i}{(k_{L_1}^2+k_{L_2}^2)^{1/2}} \frac{\pi}{\Omega} \frac{1}{(k_{L_1}^2\sin^2\alpha + k_{L_2}^2\sin^2\beta)^{1/2}}. \quad (131)$$

Furthermore the function $\tilde{\mathcal{F}}(\mathbf{K}')$ is given by Eq. (70) and $\tilde{\mathcal{P}}_1(\mathbf{K}')$ is defined by

$$\tilde{\mathcal{P}}_1(\mathbf{K}') = \exp\left\{ -\frac{\epsilon_x'^2}{2\Omega(k_{L_1}^2+k_{L_2}^2)} \frac{K_{x'}^2}{1+i\epsilon_x'^2} \right\} \times \exp\left\{ -\frac{\epsilon'^2}{2\Omega k_{L_1}^2} \frac{(\chi_c K_{y'} + \chi_{sc}K_{z'})^2}{1+i\chi_c\epsilon'^2} \right\}. \quad (132)$$

The result for $\tilde{\varrho}_F(\mathbf{K}')$ given by Eq. (127) consists of two parts: (i) a part which is only present for $m_x = m_y = 0$ and describes the Bragg-Fresnel scattering around the (0,0,0) reflection and (ii) the sum over (m_x,m_y) which describes the pure surface scattering contribution. In the following we will only discuss this surface part.

We will now again look at two limiting cases. First we note that an expansion of Eq. (127) yields in the Fraunhofer limit, i.e., in the limit $\epsilon', \epsilon_x' \gg 1 (l'k_{L_{1,2}} \to 0)$

$$\tilde{\varrho}_F(\mathbf{K}') \to \frac{l'^2}{2\pi} \frac{i\tilde{\varrho}_0}{K_{z'}} \sum_{m_x,m_y} \exp\left\{ -\frac{l'^2}{4\pi^2} (K_{x',m_x}^2 + K_{y',m_y}^2) \right\} \tilde{h}_{m_x,m_y}^{(e)}(K_{z'}), \quad (133)$$

which is the usual $\tilde{\varrho}(\mathbf{K}')$ for a periodic 2D structure of *finite* size l' in the x' and y' directions, respectively.[27]

In the extreme Fresnel limit $\epsilon', \epsilon_x' \ll 1$ Eq. (127) reduces to

$$\tilde{\varrho}_F(\mathbf{K}') = i\tilde{\varrho}_0 \sum_{m_x,m_y} \tilde{\mathcal{F}}_S(K_{x',m_x},K_{y',m_y}) \tilde{\mathcal{P}}_S(K_{x',m_x}/\Omega, \times K_{y',m_y}/\Omega) \frac{\tilde{h}_{m_x,m_y}^{(e)}(K_{y',m_y}\chi_{sc}/\chi_s K_{z''1})}{K_{y',m_y}\chi_{sc}/\chi_s + K_{z'}}, \quad (134)$$

where $\tilde{\mathcal{P}}_S(K_{x'},K_{y'})$ is given by

$$\tilde{\mathcal{P}}_S(K_{x'},K_{y'}) = \exp\left\{ -\frac{1}{4} \frac{\Delta'^2 K_{x'}^2}{(k_{L_1}^2+k_{L_2}^2)^2} \right\} \times \exp\left\{ -\frac{1}{4} \frac{\chi^2\Delta'^2K_{y'}^2}{\chi_s^2 k_{L_1}^4} \right\}, \quad (135)$$

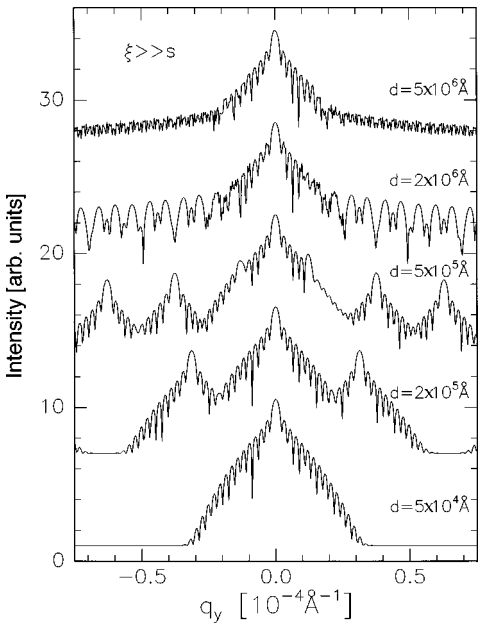

FIG. 9. The scattering from a periodic surface in the coherent limit $\xi \gg s$ and for the extreme Fresnel case ($\epsilon \approx 0.002 \ll 1$). Transverse scans for $q_{z'} = 0.1\ \text{Å}^{-1}$ along $q_{y'}$ are shown for lateral spacings d with $5\times10^4\ \text{Å} \leqslant d \leqslant 5\times10^6\ \text{Å}$.

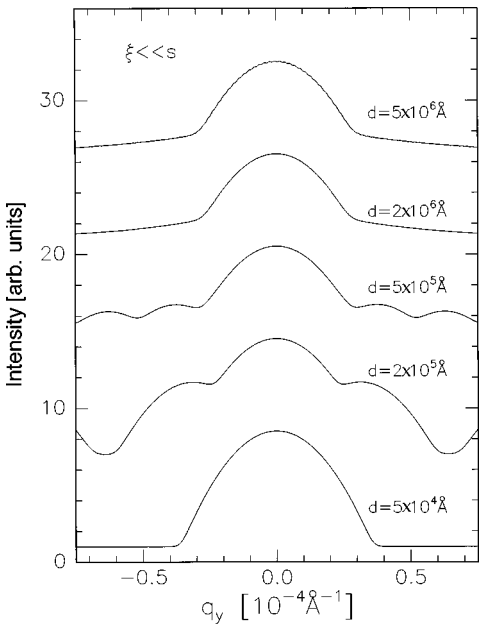

FIG. 10. The scattering from a periodic surface in the incoherent limit $\xi \ll s$. Again transverse scans for $q_{z'} = 0.1\ \text{Å}^{-1}$ along $q_{y'}$ are shown for lateral spacings d with $5\times10^4\ \text{Å} \leqslant d \leqslant 5\times10^6\ \text{Å}$.

and describes the shape of the 2D peaks at positions (q_{m_x}, q_{m_y}) in reciprocal space. Since the functions $\widetilde{\mathcal{F}}_S(\mathbf{K}')$ and $\widetilde{\mathcal{P}}_S(\mathbf{K}')$ given by Eqs. (130) and (135) are the 2D equivalents to $\widetilde{\mathcal{F}}(\mathbf{K}')$ and $\widetilde{\mathcal{P}}(\mathbf{K}')$ defined by Eqs. (70) and (100) in the case of 3D Bragg reflections, we do not have to discuss again the incoherent and coherent limits as done in Secs. IV A and IV B. However, we would like to emphasize one point where the 3D and 2D cases differ significantly. As stated at the end of Sec. IV B we saw that the oscillating quadratic terms in s_y in the final expression exactly cancel so that we got in the y direction the Fourier transform of $\Psi(s_y)$ rather than that of $\Psi(s_y)\exp\{i\Omega k_{L_1}^2 s_y^2/2\}$. If we calculate the s_y-dependent part of the product $\widetilde{\mathcal{F}}(\mathbf{K} + \Omega k_{L_1}^2 \mathbf{s})\exp\{i\Omega k_{L_1}^2 s^2/2\}$. for surfaces [see Eqs. (60) and (127)] we get

$$s_y \text{ part} \sim \exp\left\{ i\,\frac{\Omega}{2}\,\frac{k_{L_1}^2 k_{L_2}^2 \sin^2\beta}{k_{L_1}^2 \sin^2\alpha + k_{L_2}^2 \sin^2\beta}\, s_y^2 \right\} \times \exp\{(\chi/\chi_s) K_{y'} s_y \sin\alpha\}. \tag{136}$$

The linear term in s_y alone would yield in the coherent limit the Fourier transform of the aperture function $\Psi(s_y)$ as shown in Sec. IV B. However, now the s_y^2 terms do not vanish and the argument of the first exponential is of the order $k_{L_{1,2}}^2 s_y^2 \sim 1$ (for $L_{1,2} \sim 1$ m, $\lambda = 1$ Å, $s_y \sim 10\ \mu$m) and rather rapid additional oscillations are expected in the case of surface scattering.

Figures 9 and 10 show calculations of transverse scans along $q_{y'}$ for a periodic surface in the coherent and incoherent limits where we used Eqs. (60) and (127). As parameters $\lambda = 1$ Å, $L_{1,2} = 1$ m, $l' = 1$ cm, a width of the incident aperture of $s = 10\ \mu$m, and $q_{z'} = 0.1\ \text{Å}^{-1}$ were assumed. The out-of-plane direction x' was again not taken into account (see Sec. IV C). As periodic surface contour $h(x', y')$ we have chosen a rectangular shape with lateral spacing $d_{y'} = d$ and equal width of the bars and grooves for which $\widetilde{h}^{(e)}_{m_x, m_y}(K_{z'})$ may be easily calculated:

$$\widetilde{h}^{(e)}_m(K_{z'}) = \begin{cases} \exp(-iK_{z'}h_0/2)\cos(K_{z'}h_0/2) & \text{for } m = 0, \\ 0 \quad \text{for } m \text{ even} \neq 0, \\ 2/(\pi m)\exp(-iK_{z'}h_0/2)\sin(K_{z'}h_0/2) & \\ \qquad\qquad \text{for } m \text{ odd}, \end{cases} \tag{137}$$

where we set $m_y = m$ and we omit m_x. The height of the stepped surface is denoted by h_0 and was set to $h_0 = 200$ Å in the calculations. Figure 9 shows transverse scans for different lateral spacings d in the coherent limit. From the bottom to the top d increases and it can be seen that interferences occur when the peaks start to overlap (see curves for $d = 5\times10^5$ Å and $d = 2\times10^6$ Å). The curve for $d = 5\times10^4$ Å shows one single peak decorated by the aperture diffraction effects. For very large d ($d = 5\times10^6$ Å, topmost curve) the satellite peaks are very close and again one single peak is visible but weak rapid oscillations are still present throughout the whole $q_{y'}$ region.

Figure 10 shows the opposite limit, i.e., the incoherent case. Now all interference effects have vanished and only (broad) peaks are visible.[29,30] Note that for very large d ($d > 1\times10^6$ Å) only one peak is remaining since the satellites are now too close and their intensity behaves as $1/m^2$ (see Eq. 137).

B. Arbitrary surfaces

Finally we would like to discuss briefly the scattering from nonperiodic rough surfaces. Performing the limit $d_{x'}$, $d_{y'} \to \infty$ in Eqs. (127) and (129) yields $\tilde{\varrho}_F(\mathbf{K}')$ for an arbitrary nonperiodic surface contour $h(x',y')$. We get for the surface part

$$\tilde{\varrho}_F(\mathbf{K}') = i\tilde{\varrho}_0(1+i\epsilon_x'^2)^{-1/2}(\overline{\chi}\chi_s/\chi_{sc})^{1/2} \times \int\int d\tilde{K}_{x'}d\tilde{K}_{y'}\tilde{\mathcal{F}}_S(\tilde{K}_{x'},\tilde{K}_{y'}) \times \exp\left\{-\frac{\epsilon_x'^2}{2\Omega(k_{L_1}^2+k_{L_2}^2)}\frac{\tilde{K}_{x'}^2}{1+i\epsilon_x'^2}\right\} \times \exp\left\{-\frac{\epsilon'^2}{2\Omega k_{L_1}^2}\frac{\chi^2\overline{\chi}\tilde{K}_{y'}^2}{\chi_s\chi_{sc}}\right\} \times \frac{\tilde{h}^{(e)}[K_{x'}-\tilde{K}_{x'},K_{y'}-\tilde{K}_{y'};\tilde{K}_{y'}\overline{\chi}+K_{z'})}{\tilde{K}_{y'}\overline{\chi}+K_{z'}}, \tag{138}$$

where

$$\tilde{h}^{(e)}[\tilde{K}_{x'},\tilde{K}_{y'};K_{z'}] = \frac{1}{(2\pi)^2}\int\int dx'dy' \times \exp\{-iK_{z'}h(x',y'')\} \times \exp\{-i(\tilde{K}_{x'}x'+\tilde{K}_{y'}y')\}, \tag{139}$$

i.e., $\tilde{h}^{(e)}[\tilde{K}_{x'},\tilde{K}_{y'};K_{z'}]$ is the Fourier transform of $\exp\{-iK_{z'}h(x',y')\}$. We note that in the Fraunhofer limit $l'k_{L_{1,2}}^2 \to 0$ the prefactors of $\tilde{h}^{(e)}$ in Eq. (138) tend to $\to(2\pi)^2\delta(\tilde{K}_{x'})\delta(\tilde{K}_{y'})$ thus regaining the usual result for surfaces that the diffuse scattering is proportional to $\tilde{h}^{(e)}[K_{x'},K_{y'};K_{z'}]/K_{z'}$ (''truncation rod scattering'' see Refs. 21 and 25). Furthermore, we see that in Eq. (138) the combination $(\tilde{K}_{y'}\overline{\chi}+K_{z'})$ rather than $K_{z'}$ alone enters into the last argument of the function $\tilde{h}^{(e)}$. This means that a clear separation of specular and diffuse scattering in general is not possible if the incident aperture is illuminated by partially coherent radiation.

Finally we note that the results of this subsection may be easily generalized to truncation rod scattering of Bragg reflections if in Eq. (127) $\tilde{\varrho}_0$ is replaced by $\Sigma_{G'}\tilde{\varrho}(\mathbf{G}')$ and $\mathbf{K}'$ is replaced by $\delta\mathbf{K}'=\mathbf{K}'-\mathbf{G}'$ with $\mathbf{G}'$ being the locations of the Bragg reflections in reciprocal space given in surface fixed coordinates (see also Sec. IV). Recently, some systematic studies of the speckle seen in surface scattering from coherent x-ray beams have been carried out.[31]

VI. SUMMARY AND CONCLUSIONS

We have presented a general formulation (within the kinematic approximation) for the x-ray scattering from a sample characterized by an electron density distribution $\varrho(\mathbf{r})$ in terms of the mutual coherence function (MCF) of the radiation across a specified incident aperture. We have obtained the MCF of the scattered radiation across an outgoing aperture and in particular an expression for the intensity measured in a detector placed behind the outgoing aperture. The relationship between the so-called ''resolution function folding'' approach and the treatment in terms of coherence lengths is made explicit, and various limiting regimes are discussed, such as the Fraunhofer and Fresnel regimes, and for each the coherent and incoherent limits. It is shown that, except in certain cases, the observed scattering as a function of $\mathbf{q}$ cannot be interpreted simply as $|\tilde{\varrho}(\mathbf{q})|^2$ folded with an instrumental resolution function, and also that in certain regimes, the combination of coherence and finite resolution can cause scattering from different Fourier components of $\varrho(\mathbf{r})$ to interfere in reciprocal space. The results are illustrated by application to the simple cases of Bragg scattering from perfectly periodic (but finite) crystals and scattering from laterally structured surfaces, and by numerical calculations. These results illustrate that x-ray scattering experiments must in general be interpreted quantitatively with caution, after first establishing which experimental regime (Fraunhofer, Fresnel, extreme Fresnel) one is working in. The generalization of these results to the case of intensity correlation spectroscopy or time-dependent scattering will be presented in a forthcoming paper.

ACKNOWLEDGMENTS

M.T. would like to thank the German Science Foundation (DFG Contract No. To 169/2-1) and the Advanced Photon Source for financial support. This work was partially supported by the U.S. DOE under BES, Contract No. W-31-109-ENG-38. The authors thank Y.P. Feng, G. Grübel, E. Gluskin, I. McNulty, W. Press, I. K. Robinson, I. Vartanyants, and J. Wang for many helpful and stimulating discussions.

APPENDIX A

In this appendix we show how to calculate $\tilde{\varrho}_F(\mathbf{K})$ in real space with one additional standard Fourier transform. After a Fourier decomposition and truncation of the electron density $\varrho_\infty(\mathbf{r})$ of an infinite crystal by a Gaussian, the Fresnel electron density given by Eq. (30) may be written as

$$\varrho_F(\mathbf{r}) = \sum_{\mathbf{G}} \tilde{\varrho}_F(\mathbf{G})\exp\left\{i\frac{\Omega}{2}(k_{L_1}^2\mathbf{r}_{\perp,1}^2+k_{L_2}^2\mathbf{r}_{\perp,2}^2)\right\} \times \exp(i\mathbf{G}\cdot\mathbf{r})\exp(-r^2\pi^2/l^2). \tag{A1}$$

We now can use the result that for a 3D function given by

$$F(\mathbf{r}) = \exp\left(-\sum_{i,j=1}^{3} A_{ij}x_ix_j\right), \tag{A2}$$

where the A_{ij} are complex numbers, its Fourier transform is given by

$$\tilde{F}(\mathbf{K}) = \frac{\pi^{3/2}}{|\mathrm{Det}\hat{\mathbf{A}}|^{1/2}}\exp\left\{-\frac{1}{4}\sum_{i,j=1}^{3}(A_{ij}^{-1})K_iK_j\right\}. \tag{A3}$$

If we consider $\widetilde{F}(\mathbf{K}-\mathbf{G})$ instead of $\widetilde{F}(\mathbf{K})$ and a matrix $\hat{\mathbf{A}}$ defined by the arguments of the exponentials in Eq. (A1) we easily may obtain Eq. (81) as a result for $\widetilde{\varrho}_F(\mathbf{K})$ in the case of Bragg reflections.

APPENDIX B

In this appendix we will explicitly calculate the MCF at the sample position as given by

$$\Gamma_s(\mathbf{r}',\mathbf{r},0)=\int\int d\mathbf{s}\, d\mathbf{s}'\Psi(\mathbf{s})\Psi^*(\mathbf{s}')g(\mathbf{s}-\mathbf{s}') \times\exp\left\{ i\,\frac{\Omega}{2}\,k_{L_1}^2[(\mathbf{s}-\mathbf{r}_{\perp,1})^2-(\mathbf{s}'-\mathbf{r}'_{\perp,1})^2]\right\}. \tag{B1}$$

If we assume Gaussians as $g(\mathbf{s}-\mathbf{s}')$ and $\Psi(\mathbf{s})$, i.e.,

$$g(\mathbf{s}-\mathbf{s}')=\exp\left\{-\frac{(\mathbf{s}-\mathbf{s}')^2}{2\xi_t^2}\right\}, \tag{B2}$$

$$\Psi(\mathbf{s})=\exp\left\{-\frac{\mathbf{s}^2}{2\sigma^2}\right\} \tag{B3}$$

with ξ_t being the (isotropic) transverse coherence length at aperture A with size σ in the x and y directions, respectively, then the $\mathbf{s}$ and $\mathbf{s}'$ integrals may be easily evaluated yielding (with $\Omega\equiv 1$)

$$\Gamma_s(\mathbf{r}',\mathbf{r},0)=\left(\frac{2\pi\xi_t}{k_{L_1}^2\xi_s}\right)^2\exp\left\{ i\,\frac{k_{L_1}^2}{2}\,(\mathbf{r}_{\perp,1}^2-\mathbf{r}_{\perp,1}'^2)\left(1-\frac{\xi_t^2}{\xi_s^2}\right)\right\} \times\exp\left\{-\frac{1}{2\xi_s^2}\left[\frac{\xi_t^2}{\sigma^2}\,(\mathbf{r}_{\perp,1}^2+\mathbf{r}_{\perp,1}'^2) +|\mathbf{r}_{\perp,1}-\mathbf{r}'_{\perp,1}|^2\right]\right\}, \tag{B4}$$

where the definition

$$\xi_s^2=\xi_t^2\,\frac{(1+\xi_t^2/\sigma^2)^2+\xi_t^4k_{L_1}^4-1}{\xi_t^4k_{L_1}^4} \tag{B5}$$

was used. Eq. (B4) is the explicit representation of the MCF at the sample position in Gaussian approximation and Eq. (B5) is equivalent to Eq. (43) which defines the coherence length at the sample position.

[1] G. Grübel, J. Als-Nielsen, D. Abernathy, G. Vignaud, S. Brauer, G. B. Stephenson, S. G. J. Mochrie, M. Sutton, I. K. Robinson, R. Fleming, R. Pindak, S. Dierker, and J. F. Legrand, ESRF Newsletter **20**, 14 (1994).

[2] B. Lin, M. L. Schlossman, M. Meron, S. M. Williams, and P. J. Viccaro, Rev. Sci. Instrum. **66**, 1 (1995).

[3] E. Vlieg, S. A. De Vries, J. Alvarez, and S. Ferrer, J. Synchrotron Radiat. **4**, 210 (1997).

[4] M. Sutton, S. G. J. Mochrie, T. Greytak, S. E. Nagler, L. E. Berman, G. A. Held, and G. B. Stephenson, Nature (London) **352**, 608 (1991).

[5] Z. H. Cai, W. B. Lai, W. B. Yun, I. McNulty, K. G. Huang, and T. P. Russell, Phys. Rev. Lett. **73**, 82 (1994).

[6] S. B. Dierker, R. Pindak, R. M. Fleming, I. K. Robinson, and L. Berman, Phys. Rev. Lett. **75**, 449 (1995); T. Thurn-Albrecht, W. Steffen, A. Patkowski, G. Meier, E. W. Fischer, G. Grübel, and D. L. Abernathy, *ibid.* **77**, 5437 (1996); S. G. J. Mochrie, A. M. Mayes, A. R. Sandy, M. Sutton, S. Brauer, G. B. Stephenson, D. L. Abernathy, and G. Grübel, *ibid.* **78**, 1275 (1997).

[7] R. A. Shore, B. J. Thompson, and R. E. Whitney, J. Opt. Soc. Am. **56**, 733 (1966).

[8] J. E. Trebes, K. A. Nugent, S. Mrowka, R. A. London, T. W. Barbee, M. R. Carter, J. A. Koch, B. J. MacGowan, D. L. Matthews, L. B. Da Silva, G. F. Stone, and M. D. Feit, Phys. Rev. Lett. **68**, 588 (1992).

[9] H. Kaiser, S. A. Werner, and E. A. George, Phys. Rev. Lett. **50**, 560 (1983); H. Rauch, H. Wölwitsch, H. Kaiser, R. Clothier, and S. A. Werner, Phys. Rev. A **53**, 902 (1996).

[10] P. N. Pusey, in *Photon Correlation Spectroscopy and Velocimetry*, edited by H. Z. Cummins and E. R. Pike (Plenum, New York, 1977), p. 45.

[11] W. H. de Jeu, J. D. Schindler, and E. A. L. Mol, J. Appl. Crystallogr. **29**, 511 (1996).

[12] A. Gibaud, G. Vignaud, and S. K. Sinha, Acta Crystallogr., Sect. A: Found. Crystallogr. **49**, 642 (1993).

[13] A. Gibaud, J. Wang, M. Tolan, G. Vignaud, and S. K. Sinha, J. Phys. I **6**, 1085 (1996).

[14] H. Dosch, *Critical Phenomena at Surfaces and Interfaces (Evanescent X-Ray and Neutron Scattering)*, Vol. 126 of Springer Tracts in Modern Physics (Springer-Verlag, Berlin, 1992).

[15] M. Born and E. Wolf, *Principles of Optics* (Pergamon, Oxford, 1993).

[16] S. M. Durbin, Acta Crystallogr., Sect. A: Found. Crystallogr. **51**, 258 (1995).

[17] K. A. Nugent, J. Opt. Soc. Am. A **8**, 1574 (1991).

[18] K. A. Nugent and J. E. Trebes, Rev. Sci. Instrum. **63**, 2146 (1992).

[19] L. Mandel and E. Wolf, *Optical Coherence and Quantum Optics* (Cambridge University Press, Cambridge, 1995).

[20] A. C. Schell, Ph.D. thesis, MIT, Cambridge, MA, 1961.

[21] S. R. Andrews and R. A. Cowley, J. Phys. C **18**, 6427 (1985).

[22] I. K. Robinson, Phys. Rev. B **33**, 3830 (1986).

[23] B. E. Warren, Phys. Rev. **59**, 693 (1941).

[24] Here we have to mention that a Schell-model source with $\xi_x,\xi_y\equiv 0$ is not able to generate a beam (for details see Ref. 19), i.e., it would not radiate at all. However, the limit $\xi_x,\xi_y\to 0$ is not problematic in our theory.

[25] S. K. Sinha, E. B. Sirota, S. Garoff, and H. B. Stanley, Phys. Rev. B **38**, 2297 (1988).

[26] M. Tolan, G. König, L. Brügemann, W. Press, F. Brinkop, and J. P. Kotthaus, Europhys. Lett. **20**, 223 (1992).

[27] M. Tolan, W. Press, F. Brinkop, and J. P. Kotthaus, Phys. Rev. B **51**, 2239 (1995).

[28] M. Abramowitz and I. A. Stegun, *Handbook of Mathematical Functions* (Dover, New York, 1972).

[29] M. Tolan, D. Bahr, J. Süβenbach, W. Press, F. Brinkop, and J. P. Kotthaus, Physica B **198**, 55 (1994).

[30] T. Salditt, H. Rhan, T. H. Metzger, J. Peisl, R. Schuster, and J. P. Kotthaus, Z. Phys. B **96**, 227 (1994).

[31] J. L. Libbert, R. Pindak, S. B. Dierker, and I. K. Robinson, Phys. Rev. B **56**, 6454 (1997).